Research Signpost
37/661 (2), Fort P.O., Trivandrum-695 023, Kerala, India

Recent Res. Devel. Chem., 2(2004): 105-140 ISBN: 81-7736-204-6

6

The formation of σ-bonded (fullerene$^-$)$_2$ dimers and (Co^{II}TPP·fullerene$^-$) anions in ionic complexes of C_{60}, C_{70}, and $C_{60}(CN)_2$

Dmitri V. Konarev[1,2], Salavat S. Khasanov[2,3], Gunzi Saito[2] and Rimma N. Lyubovskaya[1]

[1]Institute of Problems of Chemical Physics RAS, Chernogolovka, Moscow region 142432, Russia; [2]Division of Chemistry, Graduate School of Science Kyoto University, Sakyo-ku, Kyoto 606-8502, Japan; [3]Institute of Solid State Physics RAS, Chernogolovka, 142432, Russia

Abstract

Ionic complexes of fullerenes C_{60}, C_{70}, and $C_{60}(CN)_2$ were obtained. Those are $Cp^*_2Cr·C_{60}·(C_6H_4Cl_2)_2$ (1) (Cp^*_2Cr: decamethylchromocene); $Cr(C_6H_6)_2·C_{60}·(C_6H_4Cl_2)_{0.7}$ (2), $Cr(C_6H_6)_2·C_{60}·C_6H_5CN$ (3), $Cr(C_6H_6)_2·C_{70}·C_6H_5CN$(4), ($Cr(C_6H_6)_2$: bis(benzene)chromium); $Cp_2Co·C_{60}·C_6H_4Cl_2$ (5), $Cp_2Co·C_{70}·(C_6H_4Cl_2)_{0.5}$ (6) (Cp_2Co: cobaltocene); multi-component complexes $CTV·(Cs)_2$

Correspondence/Reprint request: Dr. Dmitri V. Konarev, Division of Chemistry, Graduate School of Science Kyoto University, Sakyo-ku, Kyoto 606-8502, Japan
E-mails: konarev@kuchem.kyoto-u.ac.jp, konarev@icp.ac.ru

*·$(C_{70})_2$·$(DMF)_7$·$(C_6H_6)_{0.75}$ (**7**) and CTV·$(Cs)_2$·$(C_{60})_2$·$(DMF)_6$(**8**) containing neutral cyclotriveratrylene molecule; and multi-component complexes (D)·(Co^{II}TPP·fullerene)·Solvent (**9-14**) (Co^{II}TPP: tetraphenylporphyrinate cobalt (II); D: $Cr(C_6H_6)_2$, TDAE (tetrakis(dimethylamino)ethylene); TMA^+ (tetramethylammonium); MP^+ (N-methylpyridinium); Cs^+; and fullerene: C_{60}, and $C_{60}(CN)_2$). Fullerene radical anions were shown to have strong tendency to form diamagnetic σ-bonded $(C_{60}^-)_2$ and $(C_{70}^-)_2$ dimers in **1-8** and σ-bonded (Co^{II}TPP·fullerene$^-$) anions in **9-13**. Molecular structure of these dimers and anions were determined from X-ray diffraction analysis on single crystals. The lengths of the intercage C-C bond in the $(C_{60}^-)_2$ and $(C_{70}^-)_2$ dimers are 1.597(7) and 1.584(9) Å, whereas the lengths of the Co···C(fullerene) coordination bonds are in the 2.28-2.32 Å range. The σ-bonded anions are stable at low temperatures and dissociate above 140-250 K ($(C_{60}^-)_2$ dimer), above 250-360 K ($(C_{70}^-)_2$ dimer) and above 190-200 K (Co^{II}TPP·fullerene$^-$) anions in **12** and **13**). It was shown that stability of s-bonded anions is also defined by size of solvent molecules and cations involved in a complex. The dissociation of diamagnetic σ-bonded anions results in the increase in the magnetic moments of the complexes and the appearance of resonating EPR signals due to strong exchange coupling between non-bonded paramagnetic fullerene radical anions and cations. Peculiarities of the formation of (fullerene$^-$)$_2$ dimers, (Co^{II}TPP·fullerene$^-$) anions and other possible σ-bonded anions containing negatively charged fullerenes are discussed.*

Abbreviations

$Cr(C_6H_6)_2$: bis(benzene)chromium (0); $Cr(C_6H_5Me)_2$: bis(toluene)chromium (0); $Cr(C_6H_3Me_3)_2$: bis(mesitylene)chromium (0); Cp_2Co: cobaltocene; Cp^*_2Cr: bis(pentamethylcyclopentadienyl)chromium (II); Cp^*_2Ni: bis(pentamethylcyclopentadienyl)nickel (II); Cp^*_2Co: bis(pentamethylcyclopentadienyl) cobalt (II); Co^{II}TPP: 5, 10, 15, 20-tetraphenyl-21*H*, 23*H*-porphyrinate cobalt (II); Cr^{II}TPP: 5, 10, 15, 20-tetraphenyl-21*H*, 23*H*-porphyrinate chromium (II); Sn^{II}TpTP: 5, 10, 15, 20-tetratolyl-21*H*, 23*H*-porphyrinate tin (II); Mn^{II}TPP: 5, 10, 15, 20-tetraphenyl-21*H*, 23*H*-porphyrinate manganese (II); Fe^{II}TPP: 5,10, 15, 20-tetraphenyl-21*H*, 23*H*-porphyrinate iron (II); TDAE: tetrakis(dimethylamino) ethylene; PPN^+: bis (triphenylphosphoranylidene)ammonium cation; Ph_4P^+: tetraphenylphosphonium cation; MP^+: *N*-methylpyridinium cation; TMA^+: tetramethylammonium cation; CTV: cyclotriveratrylene; DMF; N,N`-dimethylformamide; $C_6H_4Cl_2$: *o*-dichlorobenzene; C_6H_5CN: benzonitrile; THF; tetrahydrofurane.

Introduction

Ionic complexes of fullerenes possess interesting physical properties such as superconductivity and ferromagnetism [1-3] as well as a large variety of

dimeric and polymeric structures of negatively charged fullerenes some of which also show metallic conductivity and strong magnetic correlations [4]. These structures were obtained mainly when doping fullerenes by alkali metals in a gaseous phase. The linear C_{60}^- polymer bonded by two single bonds (cyclobutane ring) was formed in metallic $M{\cdot}C_{60}$ phases (M = K, Rb, and Cs). The first phase is a three-dimensional metal down to 4 K, whereas Rb and Cs phases are one-dimensional metals undergoing metal-insulator transitions below 50 and 40 K, respectively [5-7]. The linear C_{60}^{3-} polymers bonded by one single bond were formed in Na_2RbC_{60} and Li_3CsC_{60} phases. The metallic behavior of these phases was still observed after polymerization [8, 9]. C_{60}^{4-} forms a two-dimensional polymer bonded by four single bonds in Na_4C_{60} [10]. Neutral fullerenes also form a variety of polymeric structures under high pressure and temperatures [11], some of which were doped by alkali metals [12]. Strong interest to this field of research was evoked by the discovery of high-temperature ferromagnetism in a rhombohedral polymeric C_{60} phase treated at high pressure and temperature [13]. The first σ-bonded $(C_{60}^-)_2$ dimer was found in metastable $M{\cdot}C_{60}$ phases (M = K, Rb, and Cs) and its molecular structure was for the first time studied by X-ray powder diffraction [14-17]. Neutral fullerenes also form dimers. However, in contrast to single-bonded $(C_{60}^-)_2$, in $(C_{60})_2$ and $(C_{70})_2$ dimers, fullerenes are bonded by two single bonds (cyclobutane ring) [18, 19]. Neutral $(C_{59}N)_2$ dimer formed by azafullerene is bonded by one single bond and is isoelectronic to $(C_{60}^-)_2$ dimer [20].

Most of ionic complexes of fullerenes obtained up to now by direct synthesis in solution contain monomeric fullerene radical anions. Those are $TDAE{\cdot}C_{60}$ [21], $Cp_2Co{\cdot}C_{60}{\cdot}CS_2$ [22], $Cp_2Co{\cdot}C_{60}{\cdot}C_6H_5CN$ [23], $Cp^*_2Ni{\cdot}C_{60}{\cdot}CS_2$ [24], $Cr^{III}TPP{\cdot}C_{60}{\cdot}(THF)_3$ [25], $(Cp^*_2Co)_2{\cdot}C_{60}{\cdot}(C_6H_5CN,\ C_6H_4Cl_2)_2$ [26], various salts of C_{60}^{n-} (n = 1, 2 and 3) and $C_{70}^{\bullet-}$ with PPN^+ and Ph_4P^+ [27-30], salts of C_{60}^{n-} (n = 2 and 3) with alkali metal cations [31-33], and others [34, 35]. The properties of isolated fullerene radical anions are widely discussed in literature [36].

Recently different σ-bonded polymeric and dimeric structures based on negatively charged fullerenes have been discovered in ionic complexes. A single-bonded linear C_{60}^- polymer was reported to form in ionic $Cr(C_6H_5Me)_2{\cdot}C_{60}{\cdot}CS_2$ [37]. The C_{60}^- anions form linear chains with a 9.6 Å distance between the centers and the shortest $C(C_{60})\cdots C(C_{60})$ distance of 2.12 Å, which, however, is too long for the single C-C bond. The disorder in the fullerene part does not allow this polymer to be satisfactorily characterized [37]. Linear polymer from C_{70}^{2-} was formed in $M{\cdot}C_{70}{\cdot}nNH_3$ salts (M = Ca, Sr, and Ba) and structurally characterized [38, 39]. Monomeric $C_{60}^{\bullet-}$ radical anions were shown to polymerize in a ferromagnetic phase of $TDAE{\cdot}C_{60}$ under hydrostatic pressure of 7 kbar and this polymeric phase was stable at ambient conditions. Depolymerization occurs only at heating above 520 K [40, 41].

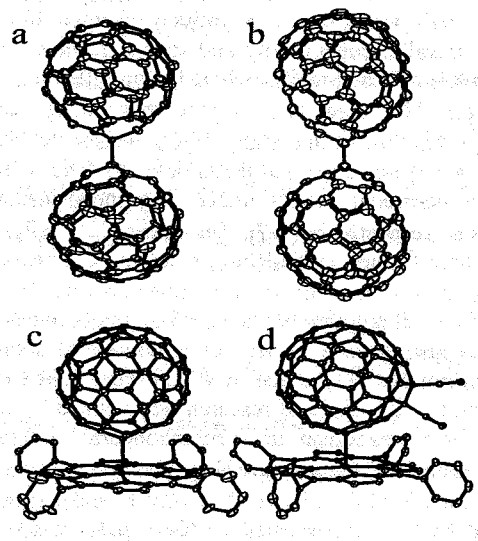

Figure 1. Molecular structure of the σ-bonded anions discussed in this review: (a) σ-bonded $(C_{60}^-)_2$ dimer; (b) σ-bonded $(C_{70}^-)_2$ dimer; (c) σ-bonded $(Co^{II}TPP{\cdot}C_{60}^-)$ anion; (d) σ-bonded $\{Co^{II}TPP{\cdot}C_{60}(CN)_2^-\}$ anion.

A reversible phase transition attributed to $C_{60}^{\bullet-}$ dimerization was observed in $Cr(C_6H_5Me)_2{\cdot}C_{60}$ at 250 K, whose crystal structure was investigated by X–ray powder diffraction [42, 43]. Recently, single crystals of an ionic C_{60}complex: $Cp^*_2Cr{\cdot}C_{60}{\cdot}(C_6H_4Cl_2)_2$ (Cp^*_2Cr, Fig. 2) have been prepared and the molecular structure of the $(C_{60}^-)_2$ dimer has been determined from X-ray diffraction on a single crystal (Fig. 1, *a*) [44]. The reversible phase transition associated with $C_{60}^{\bullet-}$ dimerization was observed in this complex at 220-200 K [44]. Similar dimers were also formed in other ionic complexes of C_{60} with $Cp^*_2Cr^+$, Cp_2Co^+, and $Cr^I(C_6H_6)_2^{\bullet+}$ (Fig. 2) [45]. $C_{60}^{\bullet-}$ is probably dimerized in $Cr^I(C_6H_3Me_3)_2{\cdot}C_{60}$ too [46]. This was concluded from the EPR, magnetic and ^{13}C NMR data. However, the complex does not show a step-like decrease of the magnetic moment with temperature, which must accompany dimerization. X-ray powder diffraction neither supports the formation of σ-bond between C_{60}^- anions at 50 K. It was assumed that the dimerization of $C_{60}^{\bullet-}$ in this complex can occur not as a first-order phase transition as it was observed in previously studied complexes but the phase transition of a higher order [46]. Related σ-bonded $(C_{70}^-)_2$ dimer (Fig. 1, *b*) was found in a multi-component complex $CTV{\cdot}(Cs)_2{\cdot}(C_{70})_2{\cdot}(DMF)_7{\cdot}(C_6H_6)_{0.75}$ (CTV, Fig.2). The preparation of single crystals of this complex allows for the first time the

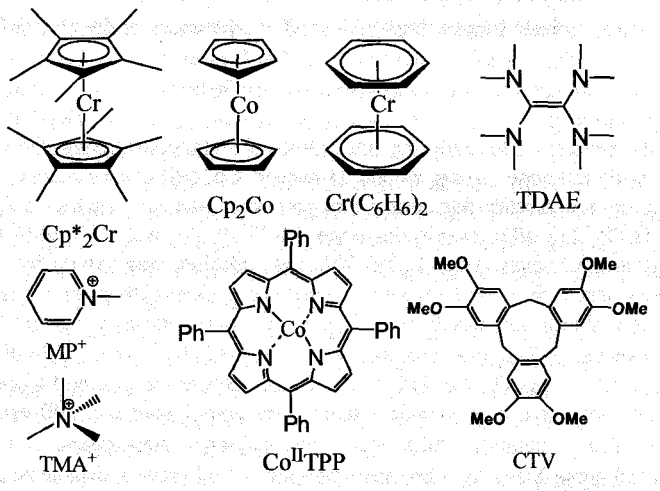

Figure 2. Molecular structures of the components used for the preparation of the ionic complexes and salts with fullerenes: decamethylchromocene (Cp^*_2Cr); cobaltocene (Cp_2Co); bis(benzene)chromium ($Cr(C_6H_6)_2$); tetrakis(dimethylamino)ethylene (TDAE); *N*-methylpyridinium (MP^+); tetramethylammonium (TMA^+); tetraphenylporphyrinate cobalt (II) ($Co^{II}TPP$); cyclotriveratrylene (CTV).

molecular structure of $(C_{70}^-)_2$ dimer to be determined [47]. Such dimers were found in other ionic complexes of C_{70} with $Cr^I(C_6H_6)_2^{\bullet+}$ [45, 48], $TDAE^+$ [49], Cp_2Co^+ [45], $Cp^*_2Cr^+$ [48], $Cp^*_2Ni^+$ [48] and Cs^+ [45]. In addition several ionic complexes of dicyanofullerene $C_{60}(CN)_2$ were obtained [50, 51], at least for one complex with $Cr^I(C_6H_6)_2^{\bullet+}$, $C_{60}(CN)_2^{\bullet-}$ was suggested to dimerize [51]. All these data show that dimerization plays an important role in ionic complexes of fullerenes.

Additionally to σ-bonded dimers formed by negatively charged fullerenes, the related family of σ-bonded ($Co^{II}TPP{\cdot}fullerene^-$) anions was found in ionic complexes containing tetraphenylporphyrinate cobalt (II) ($Co^{II}TPP$, Fig. 2) and fullerene radical anions (Fig. 1, *c* and *d*). The formation of the Co···C bond was well known and many compounds with this bond were obtained and characterized, for example, alkylcobalamins [52]. Nevertheless, the formation of σ-bonded ($Co^{II}TPP{\cdot}fullerene^-$) anions was unexpected.

Metal tetraphenyl- and octaethylporphyrins form a large variety of complexes with neutral fullerenes, their derivatives and endometallofullerenes [53-70]. These complexes (especially with porphyrins containing Co^{II}, Fe^{II} and Fe^{III}) are specified by the M···C(fullerene) contacts in the 2.55-2.70 Å range. These contacts are shorter than the sum of van der Waals radii of M and C

atoms, but essentially longer than typical M···C distances at the formation of a strong M···C bond in alkylcobalamins (1.99-2.03 Å [52]). In this case the interaction between metalloporphyrins and fullerenes can be described as secondary bonding.

It was interesting to study the interaction of metalloporphyrins, for example $Co^{II}TPP$ with fullerene radical anions. However, $Co^{II}TPP$ cannot reduce C_{60} to a radical anion due to relatively weak donor properties. Indeed, besides $Cr^{II}TPP$ [25] and $Sn^{II}TpTP$ [23], other porphyrins (even $Mn^{II}TPP$ [54] and $Fe^{II}TPP$ [60]) form only neutral complexes with C_{60} [53-70]. This problem was solved by a multi-component approach using two donor counterparts. One of them is a small-sized strong donor able to ionize fullerene (D_1), and the other one is a structure-forming neutral molecule (D_2). For example, in $[(Cr^{I}(C_6H_6)_2^{\bullet+})\cdot(Co^{II}TPP\cdot fullerene^{-})\cdot C_6H_4Cl_2]$ $Cr(C_6H_6)_2$ is D_1, $Co^{II}TPP$ is D_2, and fullerenes are C_{60}, and $C_{60}(CN)_2$. It turned out that the fullerene radical anions are bound with $Co^{II}TPP$ essentially stronger than neutral fullerenes and form diamagnetic σ-bonded ($Co^{II}TPP\cdot fullerene^{-}$) anions with shortened Co···C(fullerene$^-$) distances of 2.28-2.32 Å [72-74]. In some multi-component complexes the σ-bonded ($Co^{II}TPP\cdot fullerene^{-}$) anions can dissociate at high temperature to paramagnetic and EPR active species such as non-bonded $Co^{II}TPP$ and fullerene$^{\bullet-}$ radical anions [75] analogously to reversible dissociation of diamagnetic σ-bonded (fullerene$^-$)$_2$ dimers. The complex containing non-bonded $Co^{II}TPP$ and fullerene$^{\bullet-}$ radical anions was also obtained [76].

In this review we summarized our data on synthesis and characterization of ionic complexes of fullerenes containing σ-bonded anions of two types, namely (fullerene$^-$)$_2$ dimers and ($Co^{II}TPP\cdot fullerene^{-}$) anions. Such complexes can be interesting in several aspects:

1). the preparation of new types of σ-bonded anions based on negatively charged fullerenes (dimers, polymers, and coordination anions);
2). the structural characterization of σ-bonded anions due to availability of single crystals;
3). the changes in stability of σ-bonded anions resulting from the variation of donor and solvent molecules involved in the complex, and
4). the study of the effect of the formation of σ-bonded anions on conducting and magnetic properties of complexes.

Special attention was given in this review to structural aspects of the formation of σ-bonded anions, the effect of different factors on their stability and the changes in magnetic properties of the complexes at the transition from monomeric to dimeric phase. Finally, we discussed peculiarities of the formation of different types of σ-bonded anions.

I. Preparation of the complexes

All complexes presented in this review were obtained by the diffusion of *n*-hexane into a solution containing corresponding ionic (D_1^+) and (Fullerene$^-$) species (**1-8**) or (D_1^+), (Fullerene$^-$) and $Co^{II}TPP$ species (**9-15**) in ($C_6H_4Cl_2$), (DMF)/(C_6H_6), and C_6H_5CN)/C_6H_6 (Table 1). Slow diffusion allows the

Table 1. Characteristics of complexes **1-14** and the dissociation temperatures for the σ-bonded anions.

$(D^+)_2[(fullerene^-)_2]\cdot(Sol)_{2x}$ $(T<T_1)$ ⇄ $2[(D^+)\cdot(fullerene^{\bullet-})\cdot(Sol)_x]$ $(T>T_2)$ **(1-8)**
dimeric phase monomeric phase

$(D^+)\cdot[Co^{II}TPP\cdot fullerene^-]\cdot(Sol)_x$ $(T<T_1)$ ⇄ $(D^+)\cdot(Co^{II}TPP)\cdot(fullerene^{\bullet-})\cdot(Sol)_x$ $(T>T_2)$ **(9-14)**
σ-bonded anion non-bonded units

N	Composition of the complex	Color and shape	Dissociation temperatures for the σ-bonded anions T_1/K	T_2/K	Ref.
	Complexes containing σ-bonded $(fullerene^-)_2$ dimers				
1	$(Cp^*_2Cr^+)\cdot(C_{60}^-)\cdot(C_6H_4Cl_2)_2$	Black parallelepipeds	200	230	44,45
2	$(Cr^I(C_6H_6)_2^{\bullet+})\cdot(C_{60}^-)\cdot(C_6H_4Cl_2)_{0.7}$	Black-brown polycrystals	160	240	45
3	$(Cr^I(C_6H_6)_2^{\bullet+})\cdot(C_{60}^-)\cdot(C_6H_5CN)$	Black parallelepipeds	240	>300	45
4	$(Cr^I(C_6H_6)_2^{\bullet+})\cdot(C_{70}^-)\cdot(C_6H_4Cl_2)$	Black-brown polycrystals	250	>300	45
5	$(Cp_2Co^+)\cdot(C_{60}^-)\cdot(C_6H_4Cl_2)$	Black polycrystals	250	350	45
6	$(Cp_2Co^+)\cdot(C_{70}^-)\cdot(C_6H_4Cl_2)_{0.5}$	Black polycrystals	>300		45
7	$CTV\cdot(Cs^+)_2\cdot(C_{70}^-)_2\cdot(DMF)_7\cdot(C_6H_6)_{0.75}$	Black hexagonal plates	360	390	47
8	$CTV\cdot(Cs^+)_2\cdot(C_{60}^-)_2\cdot(DMF)_6$	Black elongated plates	140	220	
	Complexes containing σ-bonded $(Co^{II}TPP\cdot fullerene^-)$ anions				
9	$(TMA^+)\cdot(Co^{II}TPP\cdot C_{60}^-)\cdot(C_6H_5CN)\cdot(C_6H_4Cl_2)$	Black prisms	>300		76
10	$(MP^+)\cdot(Co^{II}TPP\cdot C_{60}^-)\cdot(C_6H_4Cl_2)_{1.2}$	Black prisms	>300		76
11	$(Cr^I(C_6H_6)_2^{\bullet+})_{1.7}\cdot[(Co^{II}TPP\cdot C_{60})_2^{1.7-}]\cdot(C_6H_4Cl_2)_{3.3}$	Black elongated prisms	>300		74
12	$(Cr^I(C_6H_6)_2^{\bullet+})_2(Co^{II}TPP\cdot C_{60}(CN)_2^-)\cdot(C_{60}(CN)_2^{\bullet-})\cdot(C_6H_4Cl_2)_3$	Black elongated parallelepipeds	200[a]	>300	72, 74
13	$(TDAE^{\bullet+})\cdot(Co^{II}TPP\cdot C_{60}^-)$	Black prisms	190	>300	75
14	$(Cs^+)\cdot Co^{II}TPP\cdot(C_{60}^{\bullet-})\cdot(C_6H_5CN)_{1.64}(C_6H_4Cl_2)_{0.36}\cdot CH_3CN$	Black prisms	not exists at 2 – 300 K		76

[a] - only a small contribution from non-bonded $Co^{II}TPP$ and $fullerene^{\bullet-}$ was observed.

[b] **-8** was obtained similarly to **7** [47]. The composition of **8** was determined from elemental analysis. Found, %: C = 75.36, H = 2.70, N = 3.02, 100, % - (C, H, N, %) = 18.92. Calc, %: C = 74.53, H = 2.70, N = 3.15, Cs = 10.00, O = 9.62. IR spectrum: CTV: 618w, 739w, 847w, 877w, 991w, 1031w*, 1085s*, 1142m, 1192m, 1219m, 1260s*, 1438w, 1459w, 1509m, 1606w; ($C_{60}^{\bullet-}$): 526w, 575s, 1388s; DMF: 660m, 1031w*, 1085s*, 1260s*, and 1656s (the bands marked by (*) are coincided). Visible-NIR spectrum of **8**: 336, 942, and 1074 nm ($C_{60}^{\bullet-}$).

preparation of high-quality single crystals suitable for X-ray diffraction studies. All manipulations with the complexes were made in a glove box due to air-sensitivity of the crystals. Two-component ionic complexes are unstable and decompose in air, whereas the multi-component complexes with $Co^{II}TPP$ and the same cations are essentially more stable (hours or days). All complexes were primarily characterized by IR and UV-visible spectra and then by elemental analysis, temperature dependent EPR, SQUID and conductivity measurements by a two-probe technique on a polycrystalline sample.

II. Formation of negatively charged fullerene dimers.

1. Dimerization of $C_{60}^{\bullet-}$ radical anions in $Cp^*_2Cr{\cdot}C_{60}{\cdot}(C_6H_4Cl_2)_2$ (1)

a. Structural aspects of dimerization.

In accordance with IR- and UV-visible-NIR spectra complex **1** has ionic ground state with nearly full charge transfer from Cp^*_2Cr to C_{60} molecules. $C_{60}^{\bullet-}$ exists in a monomeric form at RT. We can conclude this based on the fact that the absorption bands of neutral Cp^*_2Cr and C_{60} molecules are absent, and only the bands characteristic of $Cp^*_2Cr^+$ cations and monomeric $C_{60}^{\bullet-}$ radical anions are present in the IR-spectrum [44, 45]).

The fragment of the crystal structure of **1** at room temperature (RT) is shown in Fig. 3, *a* [45]. A direct method for structure solution (SHELX-97) gave orientationally disordered C_{60} molecules. It seems that this disorder could be approximated by freely rotating fullerene molecule. We restricted our consideration to the model of a disordered C_{60} molecule in which carbon atoms are uniformly distributed over 180 positions on the sphere found in few cycles of the Fourier synthesis. This allowed us to calculate C_{60} center-to-center distances in the structure. In contrast to $C_{60}^{\bullet-}$, $Cp^*_2Cr^+$ is completely ordered (not depicted in Fig. 3, *a*), whereas the solvent $C_6H_4Cl_2$ molecules are disordered between two orientations linked to each other by rotation about the mass center in the molecular plane. Monomeric $C_{60}^{\bullet-}$ forms uniform zig-zag chains along the diagonal to the *ac*-plane with equal center-to-center distances of 10.10 Å (10.02 Å for pristine C_{60} at RT [77]).

A reversible structural transformation accompanied by the unit cell multiplication (Table 2) takes place upon cooling **1** below 220-200 K. The zig-zag chain arrangement of C_{60}^- is still observed in a low-temperature structure at 100 K (Fig. 3, *b*). However, the center-to-center distances between C_{60}^- are not uniform. One short distance of 9.28 Å indicates the formation of σ-bonded $(C_{60}^-)_2$ dimers and the second distance of 9.91 Å is close to that between non-bonded $C_{60}^{\bullet-}$ in the RT structure. The $(C_{60}^-)_2$ dimers are statistically disordered between two orientations linked to each other by rotation of $(C_{60}^-)_2$ about the intercage C-C bond at an angle of 142°. The occupancy factors are 0.75 and 0.25.

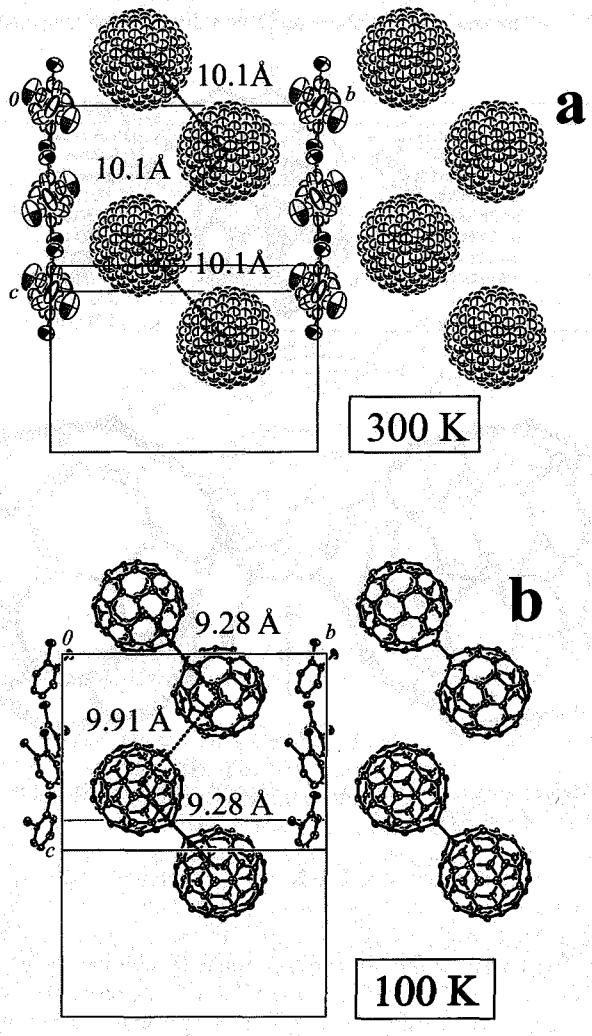

Figure 3. Two phases of the crystal structure of **1** projected onto the $C_{60}^{\bullet-}$ zig-zag chains.
(a) crystal structure at RT with monomeric orientationally disordered $C_{60}^{\bullet-}$;
(b) crystal structure at 100 K containing $(C_{60}^{-})_2$ dimers statistically disordered between two orientations (75:25). Only major orientation of $(C_{60}^{-})_2$ dimers is shown.
Reprinted with permission from [45]. Copyright 2003 American Chemical Society.

Table 2. Unit cell parameters for **1** above and below dimerization temperature (200-220 K) [44].

RT	100 K
$C_{92}H_{38}Cl_4Cr_1$	$C_{368}H_{152}Cl_{16}Cr_4$
Monoclinic	Monoclinic
Space group C2/c	Space group $P2_1$
a=23.167(5) Å	a=22.973(1) Å
b= 20.983(5) Å	b= 20.785(1) Å
c= 14.609(2) Å	c= 24.747(1) Å
β= 123.415(8)°	β= 106.387(3)°
V=5928.(2) Å^3	V=11247.7(9) Å^3
Z=4	Z=2
ρ_{calc}=1.498 g·cm^{-3}	ρ_{calc}=1.579 g·cm^{-3}

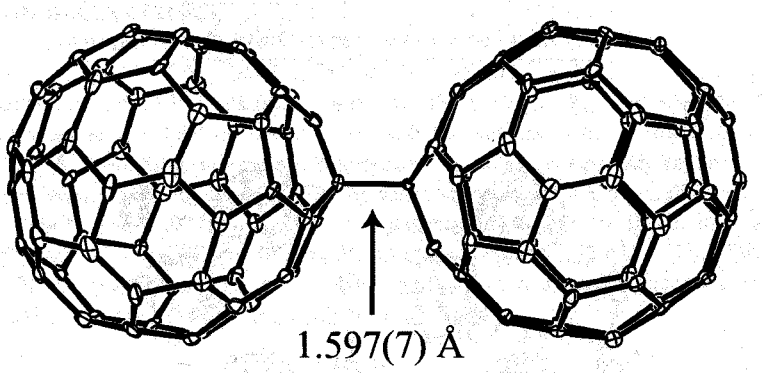

Figure 4. Molecular structure of the $(C_{60}^-)_2$ dimer determined from X-ray diffraction on a single crystal of **1** at 100 K [44].

The $(C_{60}^-)_2$ configuration at 100 K has C_{2h} symmetry with C_{60}^- arranged in *trans* conformation relative to each other, as was previously predicted [78, 79]. The average bond angle of 109° for sp^3 carbons is close to the tetrahedral geometry. The length of the 6-6 and 6-5 bonds (excluding the bonds with sp^3 carbons) was averaged to 1.391 (21) and 1.445 (21) Å, respectively. The length of the inter-cage C-C bond (1.597(7) Å) is longer than the normal C-C bond between sp^3 carbons of 1.541(3) Å [80] but close to the predicted one (1.618 Å) [79]. The intercage center-to-center distance between two C_{60}^- in the dimer is equal to 9.28 Å. This is close to the distance in a dimeric phase of Rb·C_{60} of about ~9.34 Å [16].

The single bonded $(C_{60}^-)_2$ dimer in **1** is less stable than the neutral $(C_{60})_2$ dimer with two single bonds between C_{60} of a noticeably shorter length (1.575(7) Å) [18]. Indeed, the dissociation temperature of negatively charged

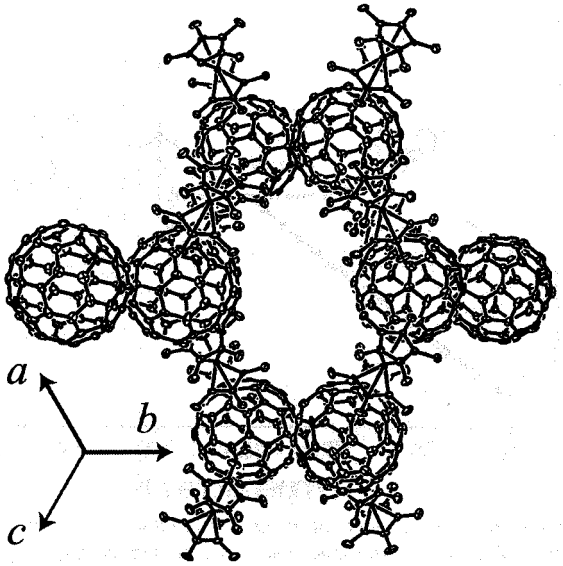

Figure 5. The projection of crystal structure of **1** at 100 K viewed along the diagonal to the *ac*-plane. The $C_6H_4Cl_2$ molecules are omitted.

$(C_{60}^-)_2$ dimer (200-220 K), is essentially lower than that of the neutral $(C_{60})_2$ dimer (423-448 K [18]). The estimated intercage C-C bond dissociation energy of 63 ± 4 kJ·mol^{-1} for the $(C_{60}^-)_2$ dimer also indicates a weakness of this bond relative to the energy for the single C-C bond in CH_3-CH_3 (the dissociation energy is 368 kJ·mol^{-1} [81]).

As a whole, the packing of the complex may be described as a honeycomb network in which $(C_{60}^-)_2$ dimers are held together by $Cp^*_2Cr^+$ cations to form large continuous channels (Fig. 5). The channels pass along the [101] direction and are occupied by the stacking $C_6H_4Cl_2$ molecules. The dimers form several shortened contacts with each other in the zig-zag chains passing along the diagonal to the *ac*-plane (the shortest C···C distance of 3.266(6) Å) and with $Cp^*_2Cr^+$ (the shortest C···C distance of 3.049(6) Å).

b. Changes in magnetic properties at dimerization

The changes in the magnetic properties of **1** can be monitored on the temperature dependence of reverse molar magnetic susceptibility measured in the 300 - 1.9 K range (Fig. 6). The estimated magnetic moment was equal to 4.20 μ_B at 300 K (μ_{eff} for the non-interacting system of S = 3/2, 1/2 spins is 4.27 μ_B) indicating the contribution of both spins from $Cp^*_2Cr^+$ (S = 3/2) and

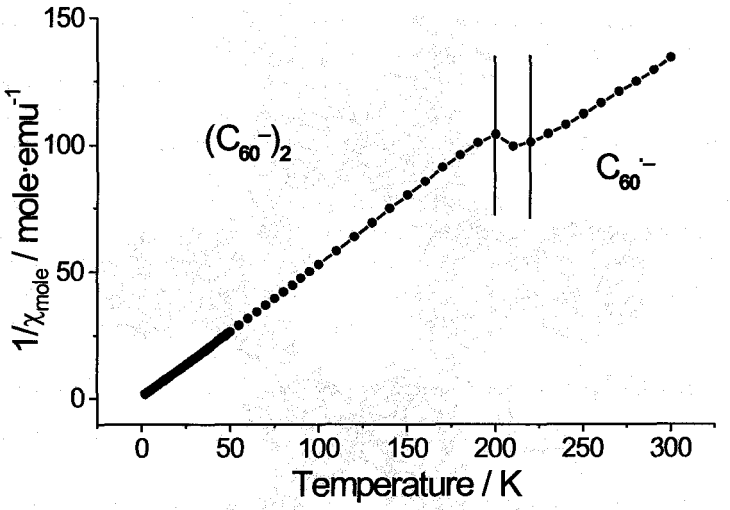

Figure 6. Temperature dependence of reverse magnetic susceptibility ($1/\chi_{mol}$) for polycrystalline **1** in the 300 - 1.9 K range. The behavior is reversible.

$C_{60}^{\bullet-}$ (S = 1/2). A close value of 4.20 μ_B was observed for ionic complex $(Cr^{III}TPP^+)\cdot(C_{60}^{\bullet-})\cdot(THF)_3$ with the same spin state (S = 3/2,1/2) [25]. A stepwise reversible decrease in the magnetic moment of **1** from 4.20 down to 3.85 μ_B was detected in the 230 - 200 K range. Below these temperatures the magnetic moment is defined by spins localized on $Cp^*_2Cr^+$ only (the μ_{eff} for the S = 3/2 system is 3.87 μ_B). The decrease of the magnetic moment of **1** indicates the disappearance of the contribution of $C_{60}^{\bullet-}$ spins (S = 1/2) accompanying the formation of the diamagnetic $(C_{60}^-)_2$ dimers. Reverse molar magnetic susceptibility shows a step-like increase at this transition at 200-220 K (Fig. 6). The dimeric phase is characterized by the Weiss constant of –1.12 K, indicating a weak antiferromagnetic interaction of spins, which results in the decrease in the magnetic moment of **1** below 30 K. However, spin ordering was not detected down to 1.9 K.

The EPR signal for **1** was not observed at RT (Fig. 7 shows the EPR spectrum of **1** at 250 K). Similarly, ionic $(Cr^{III}TPP^+)\cdot(C_{60}^{\bullet-})\cdot(THF)_3$ is EPR silent in the 300 - 4 K range [25]. It can be assumed that monomeric $C_{60}^{\bullet-}$ and $Cp^*_2Cr^+$ can give one very broad resonating signal via strong exchange coupling between these ions at RT. Upon cooling **1** below 220-200 K a new signal abruptly appears in the EPR spectrum (Fig. 7 shows this spectrum at 4 K). The signal in **1** is an asymmetric one and characterized by resonances near $g_{\perp} = 3.974$ with the line halfwidth (ΔH) of 70 G and $g_{II} = 2.013$ with $\Delta H = 55$ G

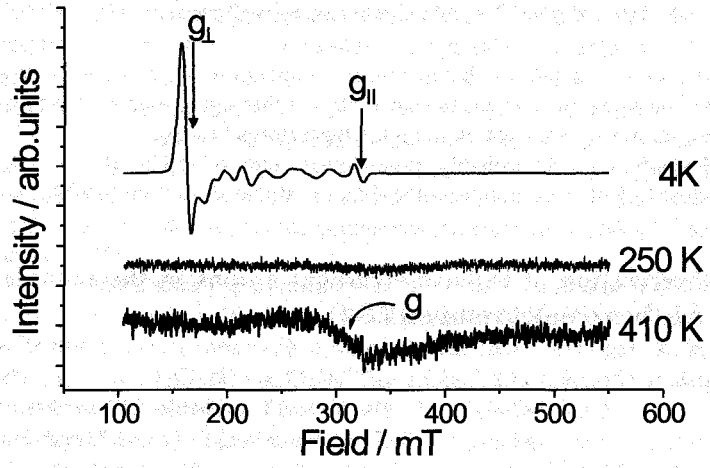

Figure 7. EPR spectrum of **1** at 4, 250 and 410 K.

at 4 K. This signal can unambiguously be ascribed to $Cp^*_2Cr^+$ with S = 3/2 ground state. Solid $(Cp^*_2Cr^+)\cdot(PF_6^-)$ produces a similar asymmetric EPR signal with $g_\perp = 4.02(1)$ and $g_{II} = 2.001(1)$ [82]. The $g_\perp$-component of the EPR signal of polycrystalline **1** is strongly asymmetric and consists of at least 9 components. The most intense component has $g_1 = 3.974$ and $\Delta H = 70$ G and each next component shifts to smaller g-factor and becomes wider (Fig. 7). The asymmetry of the EPR signal in **1** is probably a result of polycrystallinity of the sample.

The temperature of the appearance of the EPR signal from $Cp^*_2Cr^+$ in **1** correlates with the temperature of the disappearance of the contribution of the $C_{60}^{\bullet-}$ spins to magnetic susceptibility. Thus, the formation of the diamagnetic $(C_{60}^-)_2$ dimers breaks down the strong exchange coupling (observing in EPR) between spins localized on $Cp^*_2Cr^+$ and monomeric $C_{60}^{\bullet-}$ in a high temperature phase and leads to the appearance of contribution from non-interacting paramagnetic and EPR active $Cp^*_2Cr^+$ cations in a low-temperature phase.

To check the possibility of strong exchange coupling between monomeric $C_{60}^{\bullet-}$ and $Cp^*_2Cr^+$ we carried out high-temperature EPR measurements for **1** up to 410 K. Indeed, if the signal is not observed at RT and below, we are able to resolve a very broad EPR signal at temperature higher than 320 K and at high microwave power, which can be attributed to a resonating signal between $C_{60}^{\bullet-}$ and $Cp^*_2Cr^+$ ions due to strong exchange coupling. The parameters of the signal at 320 K are: g = 2.2210 and ΔH larger than 1000 G. The temperature increase noticeably narrows this signal to $\Delta H = 730$ G and shifts g-factor value

to 2.1483 (410 K). At 410 K this signal can be well resolved (Fig. 7, 410 K). Thus, the resonating EPR signal between $C_{60}^{\bullet-}$ and $Cp^*_2Cr^+$ cannot be observed at RT down to the transition temperature at 220-200 K due to essential broadening, whereas the narrowing of this signal with the temperature increase allows its observation at high temperatures (410 K).

Similarly, $C_{70}^{\bullet-}$ is probably dimerized in ionic $(Cp^*_2Cr^+)\cdot(C_{70}^-)\cdot C_6H_5Me$. According to EPR measurements the dimer is stable at least up to 300 K [48].

2. Dimerization of fullerene radical anions in the complexes with bis(benzene)chromium (2-4)

Below are discussed the following C_{60} and C_{70} complexes with bis(benzene)chromium: $Cr(C_6H_6)_2\cdot C_{60}\cdot(C_6H_4Cl_2)_{0.7}$ (**2**), $Cr(C_6H_6)_2\cdot C_{60}\cdot C_6H_5CN$ (**3**), and $Cr(C_6H_6)_2\cdot C_{70}\cdot C_6H_4Cl_2$ (**4**). The IR and UV-visible-NIR spectra of **2** - **4** indicate their ionic ground state with monomeric $C_{60}^{\bullet-}$ (**2** and **3**) and dimeric $(C_{70}^-)_2$ (**4**) at RT [45].

The data of magnetic and EPR measurements for **2** and **3** are shown in Figs. 8 and 9. The magnetic moment of **2** is 2.45 μ_B at RT and remains unchanged down to 240 K. This value is close to that calculated for the system containing two S = 1/2 spins localized on $Cr^I(C_6H_6)_2^{\bullet+}$ and $C_{60}^{\bullet-}$. The temperature dependence of reverse magnetic susceptibility in this temperature range is linear with the Weiss constant of about –17.8 K indicating a noticeable antiferromagnetic interaction of spins. The magnetic moment stepwise and reversibly decreases below 240 K down to 1.73 μ_B at 160 K (Fig. 8, *a*) (μ_{eff} for non-interacting S=1/2 system is 1.73 μ_B). Below 160 K the temperature dependence of reverse intensity is again linear however, with the essentially smaller Weiss constant of –0.51 K. Dimerization suppresses the antiferromagnetic interaction of spins observed in a high-temperature phase of the complex with monomeric $C_{60}^{\bullet-}$. Dimerization is also accompanied by the changes in the EPR spectrum. The EPR signal of **2** has g = 1.9913 at RT (Fig. 8, *b*). This value is an intermediate one between those for $Cr^I(C_6H_6)_2^{\bullet+}$ (g = 1.986 [83]) and $C_{60}^{\bullet-}$ (g = 1.998 [36]) indicating strong exchange coupling between these ions. On cooling **2** in the 240-160 K range the g-factor shifts to 1.986. This value is characteristic of non-interacting paramagnetic $Cr^I(C_6H_6)_2^{\bullet+}$ [83]. The line halfwidth monotonically decreases at dimerization (Fig. 8, *c*).

The magnetic moment of **3** is 1.74 μ_B below 230 K and remains unchanged down to 10 K. The temperature dependence of reverse molar magnetic susceptibility is also linear in this range with the Weiss constant of –0.06 K. Above 230 K the magnetic moment increases with temperature up to 2.12 μ_B at 300 K (this value is an intermediate one between 1.73 μ_B (S = 1/2) and 2.45 μ_B (S = 1/2 + 1/2)) (Fig. 9, *a*). The EPR behavior of **3** is more

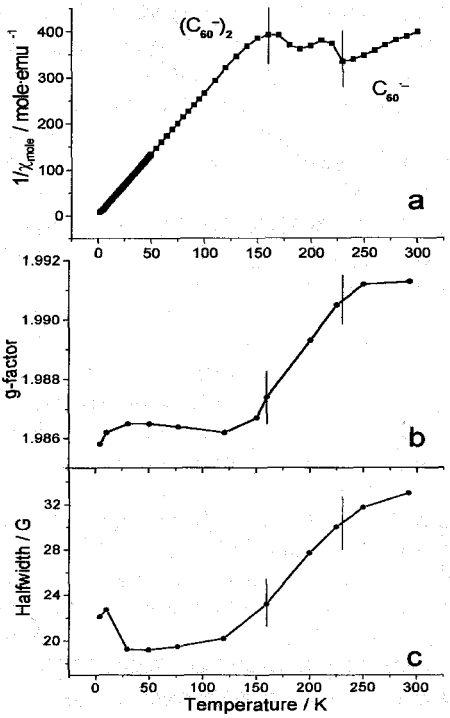

Figure 8. Data of magnetic (reverse molar magnetic susceptibility *vs* temperature (*a*)) and EPR measurements (g-factor (*b*) and the line halfwidth (*c*) for polycrystalline **2**). Figs. *b* and *c* reprinted with permission from [45]. Copyright 2003 American Chemical Society.

complicated than that of **2**. The EPR signal is a Lorentzian line with g = 1.9910 and ΔH = 30 G at RT. The g-factor shifts to 1.988 and the signal becomes narrower as in **2** with the temperature decrease down to 230 K. However, below 230 K the signal broadens and splits into two components below 150 K (g_{II} = 1.9949 and $g_{\perp}$ = 1.9835 at 4 K) (Fig. 9, *b* and *c*). Such an asymmetric signal with g_{II} = 2.0026 and $g_{\perp}$ = 1.9757 was previously observed for $Cr^{I}(C_6H_6)_2^{\bullet+}$ in rigid solution [83]. Thus, both SQUID and EPR measurements indicate dimerization of $C_{60}^{\bullet-}$ on cooling **2** and **3** in the 240 - 160 and 300 - 230 K ranges.

The magnetic moment of **4** is equal to 1.64 μ_B at 250 K and only slightly increases with temperature up to 1.78 μ_B at 300 K. The EPR signal of **4** with g = 1.9857 at RT is characteristic of $Cr^{I}(C_6H_6)_2^{\bullet+}$ [83] and does not shift with

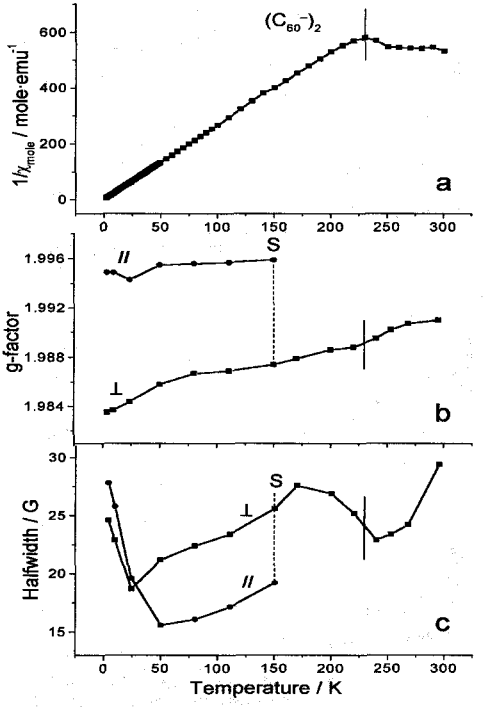

Figure 9. Data of magnetic (reverse molar magnetic susceptibility *vs* temperature (*a*)) and EPR measurements (g-factor (*b*) and the line halfwidth (*c*) for polycrystalline **3**). Figs. *b* and *c* reprinted with permission from [45]. Copyright 2003 American Chemical Society.

the temperature decrease down to 10 K. Such a behavior indicates the formation of the $(C_{70}^-)_2$ dimers and the contribution of $Cr^I(C_6H_6)_2^{\bullet+}$ spins to magnetic and spin susceptibility. The increase of the magnetic moment of **4** above 250 K suggests the beginning of dissociation of the $(C_{70}^-)_2$ dimers to paramagnetic $C_{70}^{\bullet-}$.

Some more ionic complexes of fullerenes with bis(benzene)chromium and related donors were obtained that allows one to analyze the effect of the size of solvent molecules, cations and the type of fullerene on stability of negatively charged fullerene dimers.

The size of cations can be varied using a different number of substituents in a benzene ring. The compound with the largest $Cr(C_6H_3Me_3)_2$ cation shows the lowest dissociation temperature, however $Cr(C_6H_5Me)_2$ and $Cr(C_6H_6)_2$ differing by one methyl substituent in a benzene ring have close dissociation

Table 3. Dissociation temperatures for the $(fullerene^-)_2$ dimers in ionic complexes.

Dependence on the size of cation and the type of fullerene used.

Size of cation	Complexes with C_{60} Solvent free phases	Stability	$(Fullerene^{\bullet-})\cdot(Cr(C_6H_6)_2^{\bullet+})\cdot Solv.$ Fullerene Solvent
↓	$Cr(C_6H_6)_2$ probably polymer [45, 84]* 220-300 K [51]	↓	C_{60} 220 - 300 K [51]
	$Cr(C_6H_5Me)_2$ 250 K [42, 43]		C_{70} C_6H_5Me 300 - >400 K [48]
	$Cr(C_6H_3Me_3)_2$ dimerization <170 K without phase transition [46]		$C_{60}(CN)_2$ > 380 K [51]

*- phases obtained by fast precipitation of the complex from C_6H_6 and C_6H_5Me. IR-spectra at RT show many new additional bands, which can be associated with polymerization [45].

Dependence on the size of solvent molecule.

Solvent-containing complexes of C_{60}		Solvent-containing complexes of C_{70}	
$Cr(C_6H_6)_2\cdot C_{60}\cdot CS_2$	probably polymer [37]	$Cr(C_6H_6)_2\cdot C_{70}\cdot C_6H_5Me$	300 - >400 K [48]
$Cr(C_6H_6)_2\cdot C_{60}\cdot(C_6H_4Cl_2)_{0.7}$	160 – 240 K [45]	$Cr(C_6H_6)_2\cdot C_{70}\cdot C_6H_4Cl_2$	250 - >300 K [45]
$Cr(C_6H_6)_2\cdot C_{60}\cdot C_6H_5CN$	240 – >300 K [45]		

temperatures (Table 3). An obvious tendency for stabilization of dimeric state is observed in a series: $C_{60} < C_{70} < C_{60}(CN)_2$ (Table 3). It is seen that the extension of the π-electronic system of C_{70} relatively to that of C_{60} or the introduction of two CN groups, which can to a great extent delocalize the negative charge of fullerene anions stabilize the dimeric state. Large $C_6H_4Cl_2$ solvent molecules noticeably destabilize the dimeric state relative to smaller C_6H_5CN and C_6H_5Me solvent molecules (Table 3).

3. Dimerization of fullerene radical anions in the complexes with cobaltocene (5, and 6)

Two ionic complexes of C_{60}: $Cp_2Co\cdot C_{60}\cdot CS_2$ [22], $Cp_2Co\cdot C_{60}\cdot C_6H_5CN$ [23] and one complex of C_{70}: $Cp_2Co{\sim}C_{70}$ [85] with cobaltocene obtained earlier were shown to contain monomeric $C_{60}^{\bullet-}$ [22, 23] and $C_{70}^{\bullet-}$ [85]. We prepared new C_{60} and C_{70} complexes with cobaltocene in *o*-dichlorobenzene: $Cp_2Co\cdot C_{60}\cdot C_6H_4Cl_2$ (**5**), and $Cp_2Co\cdot C_{70}\cdot C_6H_4Cl_2$ (**6**), in which fullerene radical anions are dimerized.

Complex **5** is a diamagnetic in the 1.9 - 250 K range according to SQUID measurements. This is consistent with the presence of both diamagnetic $(C_{60}^-)_2$ dimers and Cp_2Co^+ cations. Paramagnetic contribution in this temperature range corresponds to 3.3 % of S = 1/2 spins from a total amount of C_{60}. On heating **5** in the 250-350 K range, the increase in the magnetic moment up to 1.52 μ_B at 350 K is observed (Fig.10, *a*) as a result of the dissociation of the $(C_{60}^-)_2$ dimers. Above 350 K C_{60}^- exists mainly in a monomeric form. The ionic ground state of **8** with monomeric $C_{60}^{\bullet-}$ radical anions is justified by the characteristic $C_{60}^{\bullet-}$ bands in IR- and visible-NIR spectra [45].

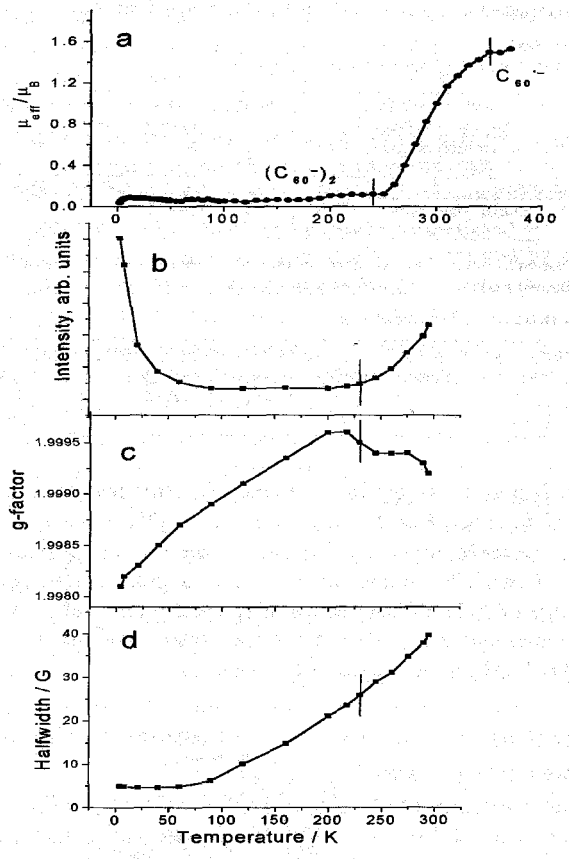

Figure 10. Magnetic moment of **5** *vs* temperature (*a*) and the data of EPR measurements (intensity (*b*), g-factor (*c*) and the line halfwidth (*d*)) for polycrystalline **5**. Figs. *a* and *b* reprinted with permission from [45]. Copyright 2003 American Chemical Society.

Two low-temperature signals were observed in the EPR spectrum of **5**. The main signal with g = 1.9979 and ΔH = 5 G at 4 K could be ascribed to $C_{60}^{\bullet-}$. The signal had weak intensity in the 1.9 - 250 K range corresponding to only 2-3 % of spins from a total amount of C_{60}. Above 250 K the intensity of the EPR signal of $C_{60}^{\bullet-}$ begins to increase (Fig. 10, *b*) together with the magnetic moment of the complex indicating the dissociation of diamagnetic $(C_{60}^-)_2$ dimers. It is interesting to note that dimerization does not almost affect

the line halfwidth of the signal and it is monotonically narrowed with the temperature decrease (Fig. 10, *d*) as in other ionic complexes with monomeric and isolated $C_{60}^{\bullet-}$ radical anions [36, 75]. At the same time the dimerization shifts g-factor to larger values (Fig 10, *c*). The second very weak and narrow EPR signal (g = 1.9998 and ΔH = 3 G) observed in the whole temperature range had temperature independent ΔH and was attributed to impurities [86].

The IR and solid state NIR spectra of **6** contain absorption bands characteristic of the $(C_{70}^{-})_2$ dimer [45]. **6** is EPR silent and shows only a weak EPR signal (< 0.1 % of total C_{70}) in the 4 - 285 K range attributable to impurities [86]. Thus, **6** contains $(C_{70}^{-})_2$ dimers from 2 up to 285 K.

4. Dimerization of fullerene radical anions in the multi-component salts 7, and 8.

Two multi-component complexes of fullerenes C_{60} and C_{70} with cesium cation and neutral cyclotriveratrylene molecule: $(Cs)_2{\cdot}(C_{70})_2{\cdot}(DMF)_7{\cdot}(C_6H_6)_{0.75}$ (**7**) and $CTV{\cdot}(Cs)_2{\cdot}(C_{60})_2{\cdot}(DMF)_6$ (**8**) are to be considered (Table 1).

Single crystal X-ray diffraction data for **7** at 120 K [47] show that C_{70}^{-} anions form σ-bonded $(C_{70}^{-})_2$ dimers. One of two crystallographically independent dimers is ordered that allows its molecular structure to be studied. Symmetry of the $(C_{70}^{-})_2$ configuration is close to C_{2h} (Fig. 11) as in the case of $(C_{60}^{-})_2$ dimer, and is lower than D_{5h} symmetry of parent C_{70}. The average bond angle for sp^3 carbons of 109° is close to tetrahedral geometry. The length of the bridging intercage C-C bonds is 1.584(9) Å and the intermolecular distance between the centers of mass of two fullerenes C_{70} is 10.417 Å. This intercage C-C bond is longer than the normal C-C bond between sp^3 carbons (1.541(3) Å) [80] and is an intermediate one between those for the negatively charged $(C_{60}^{-})_2$ and neutral $(C_{60})_2$ dimers: 1.597(7) [44] and 1.575(7) Å [18].

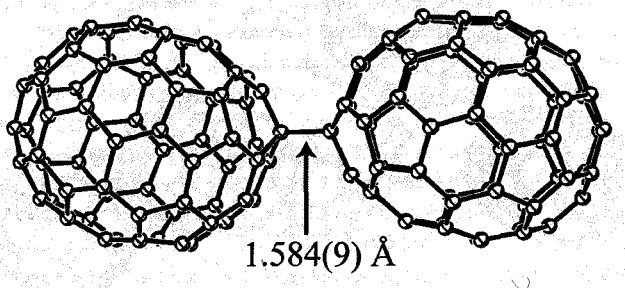

Figure 11. Molecular structure of the $(C_{70}^{-})_2$ dimer determined from the X-ray diffraction on a single crystal of **7** at 120 K [47].

Crystal structure of **7** at 120 K contains two crystallographically independent $(C_{70}^{-})_2$ dimers, two neutral CTV molecules, four cesium cations, DMF and C_6H_6 solvent molecules (Fig. 12). Such a composition of the complex results in an integer (-1) charged state of C_{70}. The complex is an example of a supramolecular array, which combines the π-π stacking of a bowl-shaped CTV molecule and an elongated C_{70} sphere together with the Cs^+ cations chelated by CTV molecules in a crown-like manner. Therefore, the neutral CTV molecules can be introduced into the $(Cs^+)\cdot(C_{70}^{-})$ salt to form a multi-component ionic compound. The π-π stacking is formed by phenylene groups of CTV and C_{70}^{-} hexagons and pentagons with shortened C…C van der Waals contacts in the 3.13 - 3.54 Å range. Multiple O(CTV)…C(C_{70}^{-}) contacts of 3.20-3.52 Å length additionally contribute to the CTV - C_{70}^{-} van der Waals interaction. The complex has a layered structure in which the layers composed of the $(C_{70}^{-})_2$ dimers alternate with those composed of CTV, Cs^+ and solvent DMF molecules. Because of this, shortened contacts between Cs^+ cations and $(C_{70}^{-})_2$ dimers are absent (>3.9 Å). However, Cs^+ cations in the layer form van der Waals contacts with CTV (each CTV molecule coordinates three Cs^+ cations with the O…Cs distances in the 3.00-3.16 Å range) and with oxygen atoms of carbonyl groups of DMF molecules with the O…Cs distances in the 2.87-3.08 Å range (Fig. 12).

Polycrystalline **7** shows a weak asymmetric EPR signal at RT having three components: $g_1 = 2.0042$ with $\Delta H = 8$ G, $g_2 = 2.0024$ with $\Delta H = 2$ G, and $g_3 = 1.9923$ with $\Delta H = 20$ G. A number of spins per a formula unit estimated from integral intensity of the EPR signal is only 0.4 % from total amoumt of C_{70}.

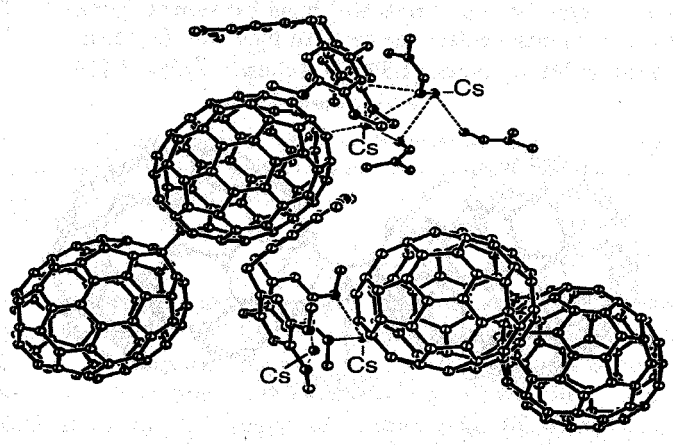

Figure 12. Fragment of crystal structure of **7**. C_6H_6 and disordered DMF molecules are omitted.

The $(C_{70}^-)_2$ dimer is diamagnetic and EPR silent, and the observed signal can be attributed to non-bonded $C_{70}^{\bullet-}$. Similar asymmetric signals are known for electro-chemically generated $C_{70}^{\bullet-}$ in solution ($g_1 = 2.007$, $g_2 = 2.003$ and $g_3 = 2.0000$ [87] and solid $(Ph_4P^+)_2(C_{70}^{\bullet-})(I^-)$ ($g_x = g_y = 1.9996$, g_z (long axis) = 2.0150, $g_{av.} = 2.0047$ [88]).

Magnetic susceptibility of **7** was measured in the 1.9 - 390 K range. The paramagnetic contribution of 2.4 % was subtracted from the experimental data revealing that magnetic susceptibility is negative at RT and is temperature independent in the 1.9 - 260 K range ($\chi_{mole} = -1.7\times10^{-3}$ emu·mole^{-1}). Thus, **7** is diamagnetic as a result of the formation of $(C_{70}^-)_2$ dimers. A small increase of magnetic susceptibility is observed in the 260-360 K range, whereas it increases abruptly above 360 K indicating the dissociation of $(C_{70}^-)_2$ (at 390 K about 90 % of dimers dissociate to $C_{70}^{\bullet-}$).

A similar complex was obtained with C_{60} (**8**). Its composition determined from elemental analysis (Table 1) is similar to that of **7**. The complex has ionic ground state with -1 charge on the C_{60} molecule as was deduced from its composition and IR- and visible-NIR spectra. Magnetic and EPR measurements indicate that below 140 K complex contains diamagnetic σ-bonded $(C_{60}^-)_2$ dimers (Fig.13) and its paramagnetic susceptibility corresponds to only ~4.6 % of spins from total amount of C_{60}. The temperature dependence of reverse molar magnetic susceptibility in this temperature range is linear with the Weiss constant of -3.4 K. The EPR signal below 140 K can unambiguously be attributed to monomeric $C_{60}^{\bullet-}$ due to characteristic narrowing of the signal with the temperature decrease and g-factor value. The estimated integral intensity of the signal is about 4 % from total amount of C_{60}. Previously we even observed EPR signals from monomeric $C_{60}^{\bullet-}$ or $C_{70}^{\bullet-}$ below dimerization temperatures in **5-7** (from 0.1 to 3 % of spins from total amount of fullerene molecules). These signals most probably were associated with a small amount of non-dimerized $C_{60}^{\bullet-}$ preserved in the sample due to a high cooling rate, the presence of defects preventing dimerization and so on. The dimers dissociate in **8** in the 140 - 220 K range. This is the lowest dissociation temperature for the $(C_{60}^-)_2$ dimers observed up to now and consequently the dimers in this complex have the lowest stability among complexes studied. Like in **5**, the dissotiation of the dimers does not change abruptly the g-factor value and ΔH (they monotonically decrease with temperature). Above 220 K C_{60}^- exists as a monomeric radical anion. It is seen that again the dissociation temperature for $(C_{60}^-)_2$ dimer in **7** is essentially lower than that for $(C_{70}^-)_2$ dimer in **8**. Similar tendency was noted for previously discussed C_{60} and C_{70} complexes with $Cp^*_2Cr^+$ (**1** and $Cp^*_2Cr\cdot C_{70}\cdot C_6H_5Me$ [48], $Cr^I(C_6H_6)_2^{\bullet+}$ (**2** and **4**), and Cp_2Co^+ (**5** and **6**).

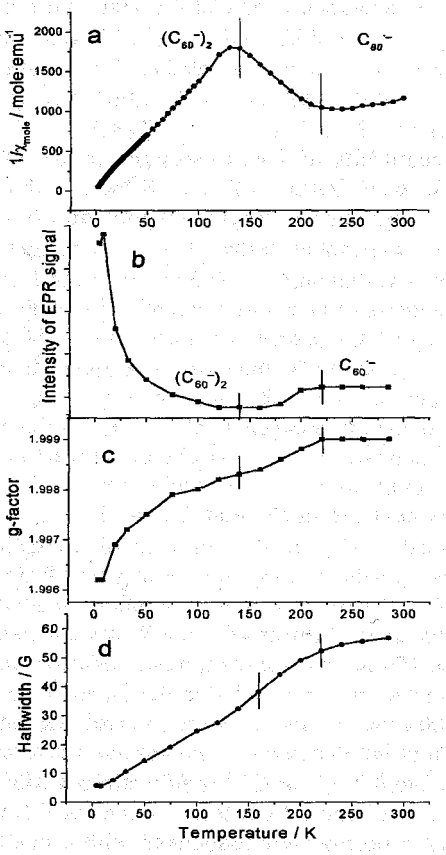

Figure 13. Data of magnetic measurements (reverse molar magnetic susceptibility *vs* temperature (*a*)) and EPR measurements (integrated intensity of EPR signal (*b*), *g*-factor (*c*), and the line halfwidth (*d*) for polycrystalline **8**).

III. The formation of σ-bonded (Co^{II}TPP·fullerene$^-$) anions.

1. Interaction of $C_{60}^{\bullet-}$ with Co^{II}TPP in ionic multi-component complexes.

A multi-component approach suggested by us was successfully used to prepare a series of complexes: $(TMA^+)\cdot(Co^{II}TPP\cdot C_{60}^-)\cdot(C_6H_5CN)\cdot(C_6H_4Cl_2)$ (**9**) [76], $(MP^+)\cdot(Co^{II}TPP\cdot C_{60}^-)\cdot(C_6H_4Cl_2)_{1.2}$ (**10**) [76], $(Cr^I(C_6H_6)_2^{\bullet+})_{1.7}\cdot$

$[(Co^{II}TPP{\cdot}C_{60})_2^{1.7-}]{\cdot}(C_6H_4Cl_2)_{3.3}$ (**11**) [74], $(TDAE^{\bullet+}){\cdot}(Co^{II}TPP{\cdot}C_{60}^{-})$ (**13**) [75], and $(Cs^+){\cdot}Co^{II}TPP{\cdot}(C_{60}^{\bullet-}){\cdot}(C_6H_5CN)_{1.64}(C_6H_4Cl_2)_{0.36}{\cdot}CH_3CN$ (**14**) [76] containing $C_{60}^{\bullet-}$ radical anions, neutral $Co^{II}TPP$ and different counter cations TMA^+, MP^+, $Cr^I(C_6H_6)_2^{\bullet+}$, $TDAE^{\bullet+}$, and Cs^+. Since bis(benzene)chromium $[Cr^0(C_6H_6)_2]$, tetrakis(dimethylamino)ethylene (TDAE) and Cs are strong donors ($E^{+/0}$ = – 0.72 V [89], – 0.75 V [90] and – 2.92 V [80], respectively), they can directly reduce C_{60} to a radical anion [74-76], whereas to introduce TMA^+ and MP^+ cations into the complexes the reaction of cationic metathesis was used [76].

The most interesting peculiarity of the crystal structure of **11** are close contacts between cobalt atom of $Co^{II}TPP$ and C_{60}^{-} carbon. There are two $(Co^{II}TPP{\cdot}C_{60}^{-})$ units, which have different Co···C(C_{60}) distances of 2.294(10) and 2.319(9) Å (Fig. 14). The Co···C(C_{60}) contacts for three other carbon atoms of C_{60} bound to coordinated carbon are 3.004 - 3.204 Å. Such coordination corresponds to the σ-bonding of $Co^{II}TPP$ to C_{60}^{-}. The 2.29-2.32 Å distances are longer than the strong covalent Co···C bond in alkylcobalamins (1.99-2.03 Å) [52] but are essentially shorter than the M···C(Fullerene) distances (in the 2.55-3.00 Å range) in the complexes of neutral fullerenes with metal-containing tetraphenyl- and Octaethylporphyrins [53-71]. As a whole, the supramolecular arrangement of **11** can be described as a cage structure with large cavities connected by channels. The walls of each cavity are built of six $(Co^{II}TPP{\cdot}C_{60}^{-})$ units. The cavities accommodate both $Cr^I(C_6H_6)_2^{\bullet+}$ cations and $C_6H_4Cl_2$ molecules [74].

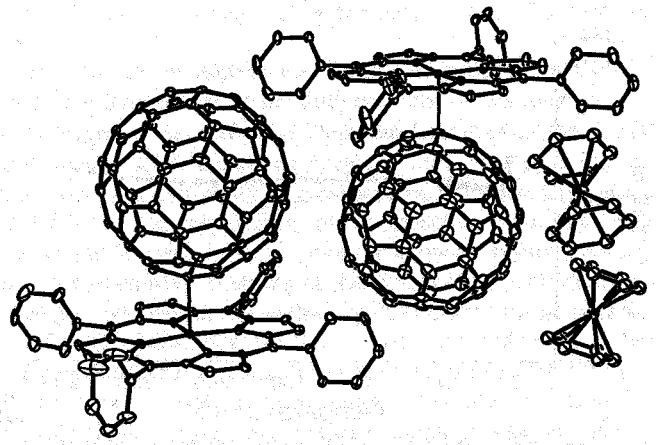

Figure 14. Fragment of crystal structure of **11**. Disordered $Cr^I(C_6H_6)_2^{\bullet+}$ with partial occupancy and $C_6H_4Cl_2$ molecules are omitted.

The magnetic moment of **11** (2.4 μ_B) is close to a calculated value for 1.7 non-interacting 1/2 spins (μ_{eff} of 2.26 μ_B) and is essentially smaller than the calculated value of 4.14 μ_B if all 5.7 non-interacting 1/2 spins from $Co^{II}TPP$, $Cr^I(C_6H_6)_2^{\bullet+}$, and ($C_{60}^{\bullet-}$) give the contribution to magnetic susceptibility. The EPR signal of **11** with g = 1.986 is characteristic of $Cr^I(C_6H_6)_2^{\bullet+}$ [83]. Thus both magnetic and EPR data show that spins in **11** are localized mainly on $Cr^I(C_6H_6)_2^{\bullet+}$ and both ($Co^{II}TPP{\cdot}C_{60}^-$) units are diamagnetic. Such a behavior is similar to that for **2-4** containing diamagnetic (fullerene$^-$)$_2$ dimers and paramagnetic $Cr^I(C_6H_6)_2^{\bullet+}$. As a result, at low temperatures these complexes have EPR signal with g-factor around 1.986 and the magnetic moment about 1.73 μ_B defined by the spins localized on $Cr^I(C_6H_6)_2^{\bullet+}$.

Complexes **9** and **10** contain diamagnetic and EPR silent TMA^+ and MP^+ cations. The absence of any EPR signals in these complexes in the 4 - 290 K range can be attributed to the formation of diamagnetic σ-bonded ($Co^{II}TPP{\cdot}C_{60}^-$) anions, which are stable at least up to 290 K [76]. Magnetic measurements support this assumption. A paramagnetic contribution to magnetic susceptibility of **9** and **10** gives only about 4 % of 1/2 spins per a formula unit. The subtraction of this paramagnetic contribution (Curie tail) from the experimental data (Fig.15) indicates that complex **10** is diamagnetic with negative temperature independent molar magnetic susceptibility of χ_{mole} = -9.5×10^{-3} emu·mole^{-1}. A similar magnetic behavior was observed for **9**. Thus the magnetic behavior of **9** and **10** is similar to that of **5-8** containing diamagnetic Cp_2Co^+ or Cs^+ cations and (fullerene$^-$)$_2$ dimers.

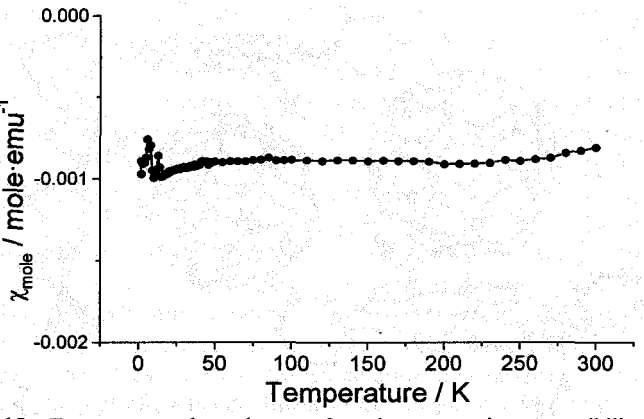

Figure 15. Temperature dependence of molar magnetic susceptibility of **10**. Diamagnetic sample holder contribution and paramagnetic contribution form Curie impurities (4 %) were subtracted from the experimental data.

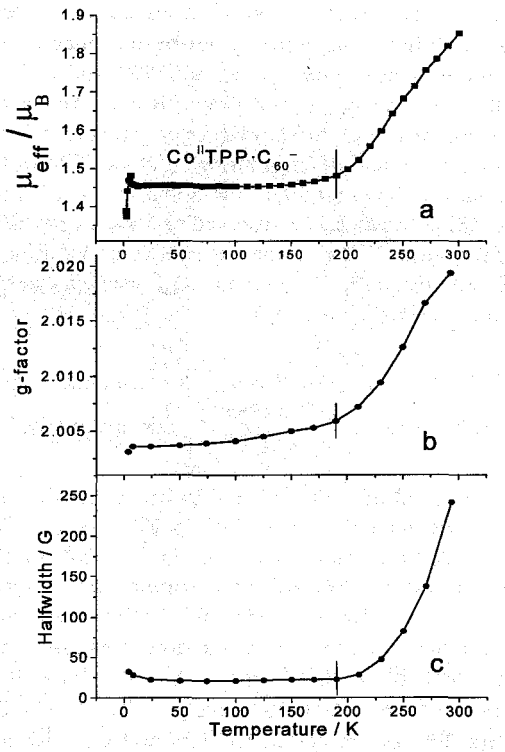

Figure 16. Magnetic moment of **13** *vs* temperature (*a*) and the data of EPR measurements (g-factor (*b*) and the line halfwidth (*c*)) for polycrystalline **13**. Fig. 16 *a*, *b* and *c* reprinted with permission from [75]. Copyright 2003 Royal Chemical Society.

Magnetic susceptibility of **13** in the 1.9 - 190 K range follows the Curie-Weiss law with the Weiss constant of 0.2 K. Since the complex formally contains three paramagnetic units with 1/2 ground state ($Co^{II}TPP$, $TDAE^{\bullet+}$ and $C_{60}^{\bullet-}$), a magnetic moment of 3 μ_B was expected. However, the observed magnetic moment is only 1.45 μ_B (Fig. 16, *a*). This value is close to that calculated for one noninteracting 1/2 spin (1.73 μ_B). The EPR spectrum of **13** in the 4 - 190 K range is a single Lorentzian line with g = 2.0030-2.0050 and nearly constant ΔH of 32 G (Fig. 16, *b* and *c*). This signal can be attributed to $TDAE^{\bullet+}$ (g = 2.0035 [91]). Thus, spins in **13** are localized mainly on $TDAE^{\bullet+}$ and the formation of diamagnetic ($Co^{II}TPP \cdot C_{60}^-$) anions in the 4 - 190 K range can be suggested.

Above 190 K, the magnetic moment of **13** increases with temperature (up to 1.85 μ_B at 300 K) (Fig. 16, *a*) probably due to the appearance of additional contribution from non-bonded paramagnetic $Co^{II}TPP$ and $C_{60}^{\bullet-}$ units to total magnetic susceptibility. This is supported by EPR data. Above 190 K the EPR signal essentially broadens and shifts to larger g-factors (g = 2.0194 and ΔH = 242 G at RT) (Fig. 16, *b* and *c*). It is known that $Co^{II}TPP$ in the complexes with neutral C_{60} and C_{70} shows a broad EPR signal with $g \cong 2.4$ and ΔH = 500-600 G at RT [54, 58]. Therefore, the observed changes in the EPR spectrum of **13** above 190 K can be attributed to the appearance of additional contribution from non-bonded paramagnetic $Co^{II}TPP$ and $C_{60}^{\bullet-}$ (which can give one broad signal due to strong exchange coupling).

σ-bonded ($Co^{II}TPP{\cdot}C_{60}^{-}$)	190 K	non-bonded $Co^{II}TPP$ and $C_{60}^{\bullet-}$
diamagnetic, EPR silent	⇄	paramagnetic, EPR active

In **11** the Co···C bond of 2.29-2.32 Å length is noticeably longer than the Co···C bond in alkylcobalamins (1.99-2.03 Å [52]) or the Co···N bond in $Co^{II}TPP{\cdot}NO$ (1.964 Å [92]). Thus σ-bonding in the ($Co^{II}TPP{\cdot}C_{60}^{-}$) anions is rather weak and the dissociation of these anions can be expected at high temperatures. Such a transition is similar to the dissociation of diamagnetic $(C_{70}^{-})_2$ and $(C_{60}^{-})_2$ dimers, which also have a rather weak intercage C-C bond. However, in case of ($Co^{II}TPP{\cdot}C_{60}^{-}$) anions their dissociation results in the appearance of other paramagnetic units, namely, $Co^{II}TPP$ and $C_{60}^{\bullet-}$.

The possibility for coexistence of $Co^{II}TPP$ and $C_{60}^{\bullet-}$ without σ-bonding was demonstrated in complex **14**. According to the composition as well as IR- and visible-NIR spectra, C_{60} molecules have nearly -1 charged state [76]. The main structural motif is a zigzag chain of alternating $Co^{II}TPP$ and $C_{60}^{\bullet-}$ (Fig. 17). Each $C_{60}^{\bullet-}$ unit forms shortened van der Waals contacts with two $Co^{II}TPP$ molecules with the shortest Co···C(C_{60}) distances in the 2.55-3.07 Å range. These contacts are of σ-type, however, they are longer than those in the σ-bonded diamagnetic ($Co^{II}TPP{\cdot}fullerene^{-}$) anions (2.28-2.32 Å [72-74]) and close to those in neutral complexes of Fe^{II}, Fe^{III} and $Co^{II}TPP$ with C_{60} (2.57-2.69 Å [60, 55, 61, 74]). Cobalt atom of $Co^{II}TPP$ does not deviate from the mean plane of the porphyrin macrocycle toward fullerene indicating the absence of noticeable Co···C($C_{60}^{\bullet-}$) bonding in **14**. On the contrary, these deviations are essentially larger (0.091-0.113 Å) in **11** and **12** containing σ-bonded ($Co^{II}TPP{\cdot}fullerene^{-}$) anions [74]. Thus, in contrast to previously described complexes, **14** contains non-bonded $Co^{II}TPP$ and $C_{60}^{\bullet-}$ units at 110 K. The EPR spectrum of **14** justifies the data of X-ray diffraction analysis. It

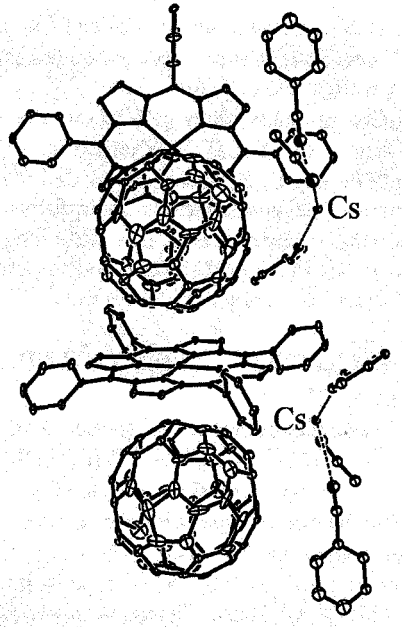

Figure 17. Fragment of crystal structure of **14**. Disordered $C_6H_4Cl_2$ molecules, which share positions with C_6H_5CN molecules are omitted.

contains two separate intense EPR signals with g = 2.0009 and 2.4982 and ΔH of 47.8 and 512 G, respectively. The first signal is attributed to the non-bonded $C_{60}^{\bullet-}$ radical anions. The line halfwidth of this signal monotonically decreases down to 3 G at 4 K. The second signal was attributed to $Co^{II}TPP$ with S = 1/2 ground state. This signal is similar to that from $Co^{II}TPP$ in the neutral complexes with fullerenes (the asymmetric signals with $g_{\perp}$ = 2.51-2.64 and ΔH = 150-300 G, g_{II} = 2.28-2.42 and ΔH = 310-450 G [54, 58, 74]). However, in contrast to neutral complexes, this is a symmetric Lorentzian line down to 4 K.

The strength of σ-bonds in ($Co^{II}TPP{\cdot}C_{60}^{-}$) anions is different in multi-component complexes discussed. Complexes **9**, **10** and **11** contain σ-bonded ($Co^{II}TPP{\cdot}C_{60}^{-}$) anions stable in the 4 – 290 K range. Evident dissociation of σ-bonded ($Co^{II}TPP{\cdot}C_{60}^{-}$) anions to non-bonded $Co^{II}TPP$ and $C_{60}^{\bullet-}$ components is observed in **13** above 190 K (about 20 % of total $Co^{II}TPP$ and $C_{60}^{\bullet-}$ exist in a non-bonded state at 290 K [75]). Complex **14** contains essentially non-bonded $Co^{II}TPP$ and $C_{60}^{\bullet-}$ components in the 4 - 290 K range.

If we consider the influence of the size of counter cations on the stability of the σ-bonded ($Co^{II}TPP{\cdot}C_{60}^{-}$) anions it is obvious that the increase in the size

of counter cations destabilizes these anions. Indeed the use of small TMA^+, MP^+, and $Cr^I(C_6H_6)_2^{\bullet+}$ cations results in stable σ-bonded anions, larger $TDAE^+$ decreases their stability, and the use of large cation like $(Cs^+)\cdot(C_6H_5CN)_2\cdot CH_3CN$ probably does not allow the close approach of $Co^{II}TPP$ to $C_{60}^{\bullet-}$ to form a $Co\cdots C(C_{60}^{\bullet-})$ σ-bond (Fig. 17). Thus, in spite of obvious ability of $Co^{II}TPP$ and $C_{60}^{\bullet-}$ to form σ-bonded $(Co^{II}TPP\cdot C_{60}^-)$ anions, steric factors also define the possibility of their formation. Similarly, the stability of σ-bonded $(C_{60}^-)_2$ dimers varies in a wide range (the beginning of the dissociation lies in the 140-250 K range) and is defined by the size of cations and solvent molecules involved in the complex.

2. Interaction of $C_{60}(CN)_2^{\bullet-}$ with $Co^{II}TPP$ in ionic multi-component complex 12

A similar multi-component complex was formed with fullerene $C_{60}(CN)_2$: $(Cr^I(C_6H_6)_2^{\bullet+})_2\cdot(Co^{II}TPP\cdot C_{60}(CN)_2^-)\cdot(C_{60}(CN)_2^{\bullet-})\cdot(C_6H_4Cl_2)_3$(**12**) [72-74]. It contains the $Co^{II}TPP\cdot(C_{60}(CN)_2^-)_2$ units at 120 K (Fig. 18). One $C_{60}(CN)_2^-$ coordinates to $Co^{II}TPP$ by the σ–type with the shortest Co…C distance of 2.283(3) Å, indicating σ-bonding. The second $C_{60}(CN)_2^-$ forms only shortened van der Waals contacts with $Co^{II}TPP$ by the η^2-type with the Co…C distances of 2.790(3) and 2.927(3) Å. These distances are close to those in the complexes of $Co^{II}TPP$ with neutral fullerenes (2.69-2.70 Å [74]). The $Co^{II}TPP\cdot(C_{60}(CN)_2^-)_2$ units form a cage structure with channels occupied by $Cr^I(C_6H_6)_2^{\bullet+}$ radical cations and $C_6H_4Cl_2$ molecules.

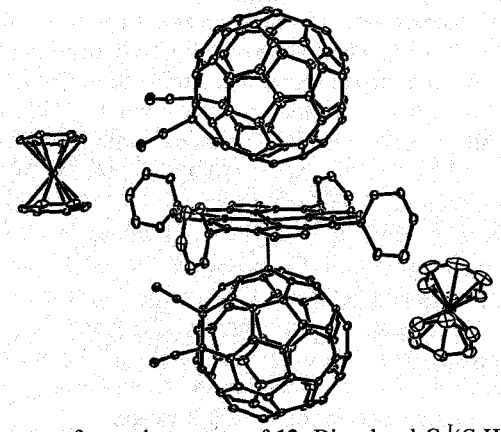

Figure 18. Fragment of crystal structure of **12**. Disordered $Cr^I(C_6H_6)_2^{\bullet+}$ with partial occupancy and $C_6H_4Cl_2$ molecules are omitted.

The magnetic moment estimated from magnetic susceptibility of **12** at RT is 2.91 μ_B. This value is close to that calculated for a system of three non interacting 1/2 spins (3.00 μ_B) and is smaller than that expected from the composition of the complex (5 units with 1/2 ground state must give magnetic moment of 3.87 μ_B). The EPR signal of **12** is a single line at RT, which is split into two components below 180 K (g_1 = 1.9821 with ΔH = 15 G and g_2 = 1.9934 with ΔH = 21 G at 4 K). These two components can be attributed to $Cr^I(C_6H_6)_2^{\bullet+}$ and non-bonded $C_{60}(CN)_2^{\bullet-}$, respectively. Therefore, three spins per a formula unit are basically localized on these ion-radicals. Consequently, the σ-bonded ($Co^{II}TPP{\cdot}C_{60}(CN)_2^-$) anions are deduced to be diamagnetic ones. Thus, in spite of the presence of two acceptor substituents on the fullerene cage $C_{60}(CN)_2^{\bullet-}$ also forms σ-bonded diamagnetic anions as parent C_{60}.

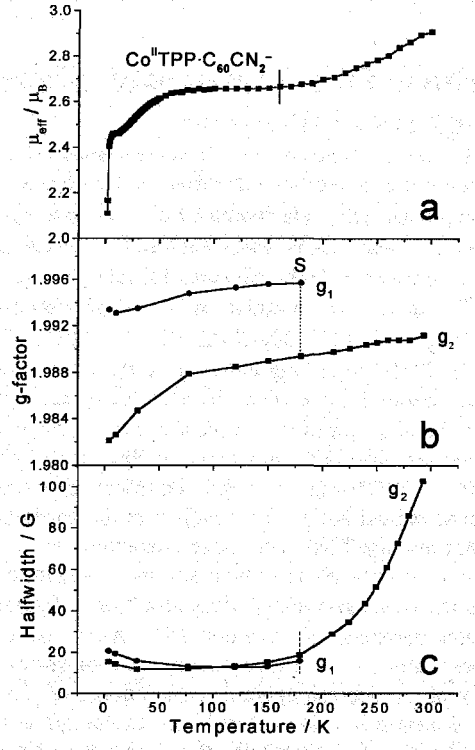

Figure 19. Magnetic moment of **12** *vs* temperature (*a*) and the data of EPR measurements (g-factor (*b*) and the line halfwidth (*c*)) for polycrystalline **12**. Fig. 19 *a*, *b* and *c* reprinted with permission from [74]. Copyright 2003 Wiley-VCH.

Careful analysis of magnetic and EPR data for **12** allows to conclude that the σ-bonded ($Co^{II}TPP{\cdot}C_{60}(CN)_2^-$) anions can begin to dissociate to non-bonded paramagnetic and EPR active $Co^{II}TPP$ and $C_{60}(CN)_2^{\bullet-}$ units above 200 K analogously to **13**. Indeed, the magnetic moment of **12** is nearly constant in the 70-200 K range (2.65 μ_B) and decrease only below 70 K due to antiferromagnetic interactions of spins. However, above 200 K the small increase of the magnetic moment is observed up to 2.91 μ_B at RT. This increase of the magnetic moment is accompanied by the essential broadening of EPR signal. Similar changes are observed at dissociation of σ-bonded ($Co^{II}TPP{\cdot}C_{60}^-$) anions in **13**. The difference only that in **13** this is accompanied by the shift of g-factor to the larger values whereas in **12** the g-factor does not shift noticeably. In any case the contribution of the non-bonded paramagnetic species in **12** at RT is smaller than that in **13**.

IV. Peculiarities of the formation of σ-bonded anions in ionic complexes of fullerenes

Direct reduction of fullerenes or metathesis reactions were used to prepare a series of new ionic complexes of fullerenes of two types. The first group involves the complexes $(D_1^+){\cdot}(fullerene^-){\cdot}Solv.$, where D_1 are $Cp^*_2Cr^+$, $Cr^I(C_6H_6)_2^{\bullet+}$, Cp_2Co^+, and $Cs^+(CTV)$. Fullerene radical anions in the compounds of the first group (**1-8**) have strong tendency to form σ-bonded $(C_{60}^-)_2$ and $(C_{70}^-)_2$ dimers in contrast to some previously studied ionic complexes ($Cp_2Co{\cdot}C_{60}{\cdot}CS_2$ [22], $Cp_2Co{\cdot}C_{60}{\cdot}C_6H_5CN$ [23], $Cp_2Co{\sim}C_{70}$ [85], and $Cp^*_2Ni{\cdot}C_{60}{\cdot}CS_2$ [24]) containing monomeric radical anions. Dimerization of fullerene radical anions is reversible and affects the magnetic properties of the complexes due to $(C_{60}^-)_2$ and $(C_{70}^-)_2$ dimers are diamagnetic. In all cases dimerization decreases magnetic moments of the complexes. Monomeric phases are specified by strong exchange coupling between paramagnetic cations and fullerene radical anions that resulted in the appearance of one EPR signal with g-factor averaged between those characteristic for non-interacting paramagnetic cations and fullerene radical anions. A negative Weiss constant indicates predominantly antiferromagnetic interactions of spins. Dimerization magnetically dilutes paramagnetic centers ($D^{\bullet+}$). As a result, the complexes containing fullerene dimers are either diamagnetic or show a paramagnetic behavior with weak antiferromagnetic interactions of spins. The other consequence of dimerization is a break of exchange coupling between paramagnetic cations and fullerene radical anions observed in a monomeric phase and the appearance of the EPR signals from isolated paramagnetic cations in the dimeric phase.

The second group involves ionic multi-component complexes: $[(D_1^+)\cdot(Co^{II}TPP)\cdot(fullerene^-)\cdot Solv.]$, which additionally to D_1 cations contain neutral $Co^{II}TPP$. In the second group, the formation of σ-bonded ($Co^{II}TPP\cdot fullerene^-$) anions has the same influence on magnetic properties of the complexes as dimerization does since σ-bonded ($Co^{II}TPP\cdot fullerene^-$) anions are also diamagnetic. Thus, their formation results in the decrease in magnetic moments and the appearance of EPR signals from paramagnetic non-interacting cations: $Cr^I(C_6H_6)_2^{\bullet+}$, and $TDAE^{\bullet+}$ instead of one resonating EPR signal (probably due to strong exchange coupling between three paramagnetic units $Co^{II}TPP$, $TDAE^{\bullet+}$, and $C_{60}^{\bullet-}$).

Stability of the dimers from negatively charged fullerenes changes in the following row: $C_{60} < C_{70} < C_{60}(CN)_2$. The introduction of acceptor substituents stabilizes the dimeric state. Possibly dimerization can play a more important role for the ionic complexes of fullerene derivatives rather than for those of parent C_{60}. All factors decreasing the repulsion between negative charges on fullerene anions in a dimer can stabilize dimeric state. Taking into account that ionic complexes with diamagnetic dimers cannot show metallic conductivity or ferromagnetism, the synthesis of fullerene based functional materials possessing such properties must be directed to destabilization of a dimeric state using, for example, electron-donating substituents. Fullerenes with extended π-electronic system as in C_{70} also have more stable dimeric state than parent C_{60}. The presence of two negative charges on the $(C_{60}^-)_2$ dimer substantially destabilizes this dimer relative to isoelectronic neutral σ-bonded $(C_{59}N)_2$ dimer formed by azafullerene. The $(C_{59}N)_2$ dimer begins to dissociate above 500 K and even at 740 K only 1 of every ~ 6000 dimers dissociates [93].

The σ-bonded ($Co^{II}TPP\cdot fullerene^-$) anions with fullerenes C_{60} and $C_{60}(CN)_2$ have nearly the same dissociation temperatures, whereas in case of $(C_{60}^-)_2$ and $(C_{60}(CN)_2^-)_2$ dimers these temperatures differ by 130 - 240 K. The repulsion between negatively charged fullerene and neutral $Co^{II}TPP$ is absent, and the delocalization of the negative charge on electron-withdrawing CN groups cannot noticeably stabilize the ($Co^{II}TPP\cdot C_{60}(CN)_2^-$) anions relative to the ($Co^{II}TPP\cdot C_{60}^-$) anions.

Sizes of solvent molecules and cations also affect stability of negatively charged dimers. Larger solvent molecules and cations must force fullerenes apart preventing the formation of intercage C-C bond and decrease dissociation temperatures for the dimers. Such effect can be reduced to simple changes in interfullerene distances. Indeed, in $Cr(C_6H_5Me)_2\cdot C_{60}$ [43], $(Cp^*_2Cr)\cdot C_{60}\cdot(C_6H_4Cl_2)_2$ (**1**) [44], and $Cr(C_6H_3Me_3)_2\cdot C_{60}$ [46] the interfullerene center-to-center distance between the C_{60}^- spheres increases in the following order: 9.986 < 10.10 < 10.124 Å (at RT). That decreases the dissociation temperatures in the following order: 250 > 200-220 > below 170 K. However,

the direct prediction of the stability of the dimers from the size of solvent molecules and cations is not possible without known crystal structures, and any correlations must be valid only in the series of related crystal structures. In ultimate case large cation and solvent molecules do not allow the formation of σ-bonded anions in spite of obvious ability of fullerene radical anions to form them. This is observed in various ionic complexes of C_{60} (see introduction) and in the multi-component complex **14**.

The ability to form σ-bonded anions is associated with the appearance of an additional electron on LUMO (π^{*1}) of fullerene radical anions. Namely this electron must take part in the formation of the intercage σ-bond. The resulted σ-bonded $(fullerene^-)_2$ dimers have an even number of π-electrons and consequently are diamagnetic. Theoretically, fullerene dianions can also form negatively charged dimers. Two electrons on the LUMO (π^{*2}) of ($fullerene^{2-}$) can take part in the σ-bonding. In this case the fullerene dianions in the dimers must be bound by two intercage σ-bonds (as in neutral fullerene dimer). Such dimer is a diamagnetic one. The repulsion between two negative charges in the dimer destabilizes the dimeric state. Because of this, it can be expected that the dimers composed of fullerene anions with charged state higher than –1 can be less stable than corresponding $(fullerene^-)_2$ dimers.

The formation of ($Co^{II}TPP{\cdot}fullerene^-$) anions is closely related to the dimerization of fullerene radical anions. However, in this case the LUMO of fullerene radical anions interacts with the d_{Z^2} orbital of $Co^{II}TPP$ producing one molecular orbital (MO) capable of σ-bonding with metal d_{Z^2}. Since fullerene radical anion has one electron on LUMO (π^{*1}) and $Co^{II}TPP$ (d^7) has one electron on d_{Z^2} orbital, the σ MO is occupied by two electrons. A two-electron covalent bond between Co and $fullerene^{\bullet-}$ is formed resulting in diamagnetism of the ($Co^{II}TPP{\cdot}fullerene^-$) anions. It should be noted that covalently bonded $Co^{II}TPP{\cdot}NO$ with a similar electronic configuration ($Co^{II}TPP$ (d^7), and NO (π^{*1})) is also diamagnetic and EPR silent [94]. Provided that $Co^{II}TPP$ (d^7) interacts with ($fullerene^{2-}$) (π^{*2}), one more additional electron must be added to the MO scheme. This electron can be placed even to π* orbital of fullerene. Such ($Co^{II}TPP{\cdot}fullerene^{2-}$) anion should also have similar σ- (Co···C) bonding but a doublet (S = 1/2) ground state.

Acknowledgements

The work was partly supported by a Grant-in-Aid Scientific Research from the Ministry of Education, Culture, Sports, Science and Technology, Japan (152005019, 21st Century COE, and Elements Science 12CE2005) and the RFBR grants N 03-03-32699). The authors would like to thank Dr. Y. Yoshida for the synthesis of $C_{60}(CN)_2$.

References

1. Rosseinsky, M.J. 1995, J. Mater. Chem., 5, 1497.
2. Gotschy, B. 1996, Fullerene Sci. and Technol., 4, 677.
3. Konarev, D.V., Lyubovskaya, R.N. 1999, Russ. Chem. Rev., 68, 19.
4. Prassides, K. 2000, The Physics of fullerenes-based and fullerene-related materials, W. Andreoni (Ed.), Kluwer Academic Publishers, Netherlands), 175.
5. Stephens, P.W.; Bortel, G.; Faigel, G.; Tegze, M.; Jánossy, A.; Pekker, S.; Oszlanyi, G.; Forró, L. 1994, Nature, 370, 636.
6. Bommeli, F., Degiory L., Wacher, P., Legeza, O., Janossy, A., Oszlanyi, G., Chauet, O, and Forró, L. 1995, Phys. Rev. B, 51, 14794.
7. Btouet, V., Alloul, H., Yoshinary, Y., and Forró, L. 1996, Phys. Rev. Lett., 76, 3638.
8. Bendele, G., Stephens, P., Prassides, K., Vavekis, K., Kortados, K., and Tanigaki, K. 1998, Phys. Rev. Lett., 80, 736.
9. Margadonna, S., Prassides, K., Knudsen, K., Hanfland, M., Kosaka, M., and Tanigaki, K. 1999, Chem. Mater., 11, 2960.
10. Oszlányi, G., Baumgarther, G., Faigel, G., and Forró, L. 1997, Phys. Rev. Lett., 78, 4438.
11. Blank, V.D., Buga, S.G., Dubitsky, G.A., Serebryanaya, N.S., Popov, M.Yu., and Sundqvist, B. 1998, Carbon, 36, 319.
12. Winter, J., Kuzmany, H., Soldatov, A., Persson, P., Jacobsson, P., and Sundqvist, B. 1996, Phys. Rev. B., 54, 17486.
13. Makarova, T.L., Sandqvist, B., Höhne, R., Esquinaz, P., Kopelevich, Y., Scharff, P., Davydov, V.A., Kashevarova, L.S., and Rakhmanina, A.R. 2001, Nature, 413, 716.
14. Zhu, Q., Cox, D.E., and Fischer, J.E. 1995, Phys. Rev. B, 51, 3966.
15. Oszlányi, G., Bortel, G., Faigel, G., Tegze, M., Grárásy, L., Pekker, S., Stephens, P.W., Bendele, G., Dinnebier, R., Mihály, G., Jánossy, A., Chauvet, O., and Forró, L. 1995, Phys. Rev. B, 51, 12228.
16. Oszlányi, G., Bortel, G., Faigel, G., Gránásy, L., Bendele, G., Stephens, P.W., and Forró, L. 1996, Phys. Rev. B, 54, 11849.
17. Kosaka, M., Tanigaki, K., Tanaka, T., Atake, T., Lappas, A., Prassides, T. 1995, Phys. Rev. B, 51, 12018.
18. Wang, G-W., Komatsu, K., Murata, Y., and Shiro, M. 1997, Nature, 387, 583.
19. Forman, G.S., Tagmatarchis, N., Shinohara, H., 2002, J. Am. Chem. Soc., 124, 178.
20. Hummelen, J.C., Khight, B., Pavlovich, J., Gonzales, R., and Wudl. F. 1995, Science, 269, 1554.
21. Allemand, P.-M., Khemani, K.C., Koch, A., Koch, A., Wudl, F., Holczer, K., Donovan, S., Grüner, G., and Thompson, J.D. 1991, Science, 253, 301.
22. Balch, A.L., Lee, J.W., Noll, B.C., and Olmstead, M.M. 1994, Recent Advances in the Chemistry and Physics of Fullerenes and Related Materials», K.M. Kadish, R.S. Ruoff (Eds.), 24, 1231.
23. Stinchcombe, J., Pénicaud, A., Bhyrappa, P., Boyd, P.D.W., and Reed, C.A. 1993, J. Am. Chem. Soc., 115, 5212.

24. Wan, W.C., Liu, X., Sweeney, G.M., and Broderick, W.E., 1995, J. Am. Chem. Soc., 117, 9580.
25. Pénicaud, A., Hsu, J., Reed, C.A., Koch, A., Khemani, K., Allemand, P.-M., and Wudl, F. 1991, J. Am. Chem. Soc., 113, 6698.
26. Konarev, D.V., Khasanov, S.S., Vorontsov, I.I., Saito G., Antipin, Yu.M., and R.N. Lyubovskaya, 2003, Inorg. Chem., 42, 3706.
27. Penicaud A., Perez-Benitez, A., Gleason, R., Munoz P, E., and Escudero, R., 1993, J. Am. Chem. Soc., 115, 10392.
28. Bilow, U., and Jansen, M. 1994, J. Chem. Soc., Chem. Commun., 403.
29. Paul, P., Xie, Z., Bau, R., Boyd, P.D.W., and Reed, C.A. 1994, J. Am. Chem. Soc., 116, 4145.
30. Penicaud, A., Perez-Benitez, A., Escudero, R., and Coulon, C., 1995, Solid State Commun., 96, 147.
31. Fässler, T.F., Spiekermann, A., Spahr, M.E., and Nesper, R. 1997, Angew. Chem., Int. Ed., 36, 486.
32. Fässler, T.F., Hoffmann, R., Hoffmann, S., and Wörle, M. 2000, Angew. Chem., Int. Ed, 39, 2091.
33. Janiak. C., Mühle, S., Hemling, H. 1995, Polyhedron, 15, 1559.
34. Himmel, K., and Jansen, M. 1998, Eur. J. Inorg. Chem., 1183.
35. Himmel, K. and Jansen, M. 1998, Chem. Commun., 1205.
36. Reed, C.A., and Bolskar, R.D. 2000, Chem. Rev., 100, 1075.
37. Broderick, W.E., Choi, K.W., and Wan, W.C. 1997, Electrochemical Soc. Proc., 14, 1102.
38. Brumm, H., Peters, E., and Jansen, M. 2001, Angew. Chem. Int. Ed., 40, 2069.
39. Wedig, U., Brumm, H., and Jansen, M. 2002, Chem. Eur. J. 8, 2769.
40. Mizoguchi, K., Machino, M., Sakamoto, H., Kawamoto, T., Tokumoto, M., Omerzy, A., and Mihailovic, D. 2001, Phys. Rev. B, 63, 140417.
41. Garaj, S., Kambe, T., Forró, L., Sienkiewicz, A., Fujiwara, M., and Oshima, K. 2003, Phys. Rev. B, 68, 144430.
42. Hönnerscheid, A., Wüllen, L., Jansen, M., Rahmer, J., and Mehring, M. 2001, J. Chem. Phys., 115, 7161.
43. Hönnerscheid, A., Dinnebier, R., and Jansen, M. 2002, Acta. Crystallogr. Sect. B, 58, 482.
44. Konarev, D.V., Khasanov, S.S., Otsuka, A., and Saito, G. 2002, J. Am. Chem. Soc., 124, 8520.
45. Konarev, D.V., Khasanov, S.S., Saito, G., Otsuka, A., Yoshida, Y., and Lyubovskaya, R.N. 2003, J. Am. Chem. Soc, 125, 10074.
46. Hönnerscheid, A., van Wüllen, L., Dinnebier, R., Jansen, M., Rahmer, J., and Mehring, M. 2004, Phys. Chem. Phys., 6, 2454.
47. Konarev, D.V., Khasanov, S.S., Vorontsov, I.I., Saito, G., Antipin, Yu.A., Otsuka, A., and R.N. Lyubovskaya, 2002, Chem. Commun., 2548.
48. Yoshida, Y., Otsuka, A., Konarev, D.V., and Saito, G. 2003, Synth. Met., 133-134, 703.
49. Oshima, K., Kambe, T., Fujiwara, M., Nogami, Y. 2003, Synth. Met., 133-134, 609.
50. Suo, Z., Wei, X., Zhou, K., Zhang, Y., Li, C., and Xu, Z. 1998, J. Chem. Soc., Dalton Trans., 3875.

51. Yoshida, Y., Otsuka, A., Drozdova, O.O., Yakushi, K., Saito, G., 2003, J. Mater. Chem., 13, 252.
52. Rossi, M., Glusker, J.P., Randaccio, L., Summers, M.F., Toscano, P.J., and Marzilli, L.G. 1985, J. Am. Chem. Soc. 107, 1729.
53. Olmstead, M.M., Costa, D.A., Maitra, K., Noll, B.C., Phillips, S.L., Van Calcar, P.M., and A.L. Balch, 1999, J. Am. Chem. Soc. 121, 7090.
54. Yudanova, E.I., Konarev, D.V., Gumanov, L.L., and Lyubovskaya, R.N. 1999, Russ. Chem. Bull., 48, 718.
55. Evans, D.R., Fackler, N.L.P., Xie, Z., Rickard, C.E.F., Boyd, P.D.W., and C.A. Reed, 1999, J. Am. Chem. Soc. 121, 8466.
56. Boyd, P.D.W., Hodgson, M.C., Rickard, C.E.F., Oliver, A.G., L. Chaker, P.J. Brothers, Bolskar, R.D., Tham, F.S., and Reed, C.A. 1999, J. Am. Chem. Soc. 121, 10487.
57. Ishii, T., Aizawa, N., Yamashita, M., Matsuzaka, H. Kodama, T., Kikuchi, K. Ikemoto, I. Iwasa, Y. 2000, J. Chem. Soc., Dalton Trans., 4407.
58. Konarev, D.V., Neretin, I.S., Slovokhotov, Yu.L., Yudanova, E.I., Drichko, N.V., Shul`ga,Yu. M., Tarasov, B.P., Gumanov, L.L., Batsanov, A.S., Howard, J.A.K., and Lyubovskaya, R.N. 2001, Chem. Eur. J., 7, 2605.
59. Konarev, D.V., Yudanova, E.I., Neretin, I.S., Slovokhotov, Yu.L., and Lyubovskaya, R.N. 2001, Synth. Met., 121, 1119.
60. Mikami, S., Sugiura, K., Asato, E., Maeda, Y., and Sakat, Y. The Proceeding of the conference "The 19th Fullerene General Symposium", Kiryu, Japan, July 27-28, 2000, p. 40.
61. Ishii, T., Kenehama, R., Aizawa, N., Yamashita, M., Matsuzaka, H., Sugiura, K., Miyasaka, H., Kodama, T., Kukuchi, K., Ikemoto, I., Tanaka, H., Marumoto, K., and Kuroda S., 2001, J. Chem. Soc., Dalton Trans., 2975.
62. Konarev, D.V., Kovalevsky, A.Yu., Li, X., Neretin, I.S., Litvinov, A.L., Drichko, N.V., Slovokhotov, Yu.L., Coppens, P., and Lyubovskaya, R.N. 2002, Inorg. Chem., 41, 3638.
63. Litvinov, A.L., Konarev, D.V., Kovalevsky, A. Yu., Coppens, P., and Lyubovskaya, R.N. 2003, CrysEngCommun., 5, 137.
64. Litvinov, A.L., Konarev, D.V., Kovalevsky, A.Yu., Lapshin, A.N., Drichko, N.V., Yudanova, E.I., Coppens, P., and Lyubovskaya, R.N. 2003, Eur. J. Inorg. Chem., 3914.
65. Konarev, D.V., Neretin, I.S., Litvinov, A.L., Drichko, N.V., Slovokhotov, Yu. L., Lyubovskaya, R.N., Howard, J.A.K., and Yufit, D.S., 2004, Cryst. Growth Des., 4, 643.
66. Ishii, T., Aizawa, N., Kanehama, R., Yamashita, M., Sugiura, K., and Miyasaka, H. 2002, Coordination Chem. Rev., 226, 113.
67. Konarev, D.V., Khasanov, S.S., Saito, G. and Lyubovskaya. R.N. 2003, J. Porph. Phth., 7, 801.
68. Stevenson, S., Rice, G., Glass, T., Harich, K., Cromer, F., Jordan, M.R., Craft, J., Hadju, E., Bible, R., Olmstead, M.M., Maitra, K., Fisher, A.J., Balch, A.L., and Dorn, H.C. 1999, Nature, 401, 55.
69. Olmstead, M.M., Bettencourt-Dias, A., Duchamp, J.C., Stevenson, S., Marciu, D., Dorn, H.C. and Balch. A.L. 2001, Angew. Chem. Inter Ed. 40, 1223.

70. Olmstead, M.M., Bettencourt-Dias, A., Duchamp, J.C., Stevenson, S., Dorn, H.C., and Balch, A.L. 2000, J. Am. Chem Soc., 122, 12220.
71. Olmstead, M.M., Lee, H.M., Dorn, H.C., and Balch, A.L. 2002. Commun., 2688.
72. Konarev, D.V., Khasanov, S.S., Otsuka, A., Yoshida, Y., and Saito, G. 2002, J. Am. Chem. Soc., 124, 7648.
73. Konarev, D.V., Khasanov, S.S., Otsuka, A., Yoshida, Y., and G. Saito, 2003, Synth. Met., 133-134, 707.
74. Konarev, D.V., Khasanov, S.S., Otsuka, A., Yoshida, Y., Lyubovskaya, R.N., and Saito, G. 2003, Chem. Eur. J., 9, 3837.
75. Konarev, D.V., Neretin, I.S., Saito, G., Slovokhotov, Yu.L., Otsuka, A., and Lyubovskaya, R.N., 2003, Dalton Trans., 3886.
76. Konarev, D.V., Neretin, I.S., Saito, G., Slovokhotov, Yu.L., Otsuka, A., and Lyubovskaya, R.N. 2004, Eur. J. Inorg. Chem., 1794.
77. Heiney, P.A., Fischer, J.E., McGhie, A.R., Romanov, W.J., Denenstein, A.M., McCauley Jr., J.P., Smith III, A.B., and Cox, D.E. 1991, Phys. Rev. Lett., 67, 1468.
78. Kürti, J., and Németh, K. 1996, Chem. Phys. Lett. 256, 119.
79. Lee, K.H., Park, S.S., Suh, Y., Yamabe, T., Osawa, E., Lüthi, H.P., Gutta, P., and Lee, C. 2001, J. Am. Chem. Soc. 123, 11085.
80. Kennard, O.1987, CRC Handbook of chemistry and physics, R.C. Weast, (Ed.), CRC Press, Inc. Boca Raton, Florida), F 106.
81. Benson, S.W. 1965, J. Chem. Ed., 42, 502.
82. Robbins, J.L., Edelstein, N., Spencer, B., and Smart, J.C. 1982, J. Am. Chem. Soc., 104, 1882.
83. Elschenbroich, C., Bilger, E., and Koch, J. 1984, J. Am. Chem. Soc., 106, 4297
84. Kaplunov, M.G., Golubev, E.V., Kulikov, A.V., and Spitsina, N.G. 1999, Izv. Acad. Nauk, Ser. Khim., 785.
85. Mrzel, A., Umek, P., Cevk, P., Omerzu. A., and Mihailovic, D. 1998, Carbon, 36, 603.
86. Paul, P., Bolskar, R.D., Clark, A.M., and Reed, C.A. Chem. Commun., 2000, 1229.
87. Dubois, D., and Kadish, K.M. 1991, J. Am. Chem. Soc., 113, 4364.
88. Pénicaud, A. Peréz-Benítez, A., Escudero R. and Coulon, C. 1995, Solid State Commun, 96, 147.
89. Treichel, P.M., Essenmacher, G.P., Efner, H.F., and Klabunde, K.J. 1981, Inorg. Chim. Acta, 48, 41.
90. Saito, G., Teramoto, T., Otsuka, A., Sugita, Y., Ban, T., Kusunoki, M., and Sakaguchi, K., 1994, Synth. Met., 64, 359.
91. Kuwata K., and Geske, D.H. 1964, J. Am. Chem. Soc., 86, 2101.
92. Scheidt, W.R., Hoard, J.L. 1973, J. Am. Chem. Soc. 95, 8281.
93. Simon, F.D., Arčon, D., Tagmatarchis, N., Garaj, S., Forro, L., and Prassides, K.; 1999, J. Phys. Chem. A, 103, 6969.
94. Wayland, B.B., Minkiewicz, J.V., Abd-Elmageed, M.E. 1974, J. Am. Chem. Soc., 96, 2795.